Optical response functions with semiclassical dynamics

W. G. Noid, Gregory S. Ezra, and Roger F. Loring
Department of Chemistry and Chemical Biology, Baker Laboratory, Cornell University, Ithaca, New York 14853

(Received 6 February 2003; accepted 3 April 2003)

Observables in nonlinear spectroscopic measurements may be calculated from response functions, which have the form of averages of nested commutators involving the operator governing the radiation–matter interaction. We present a semiclassical formulation of the optical nonlinear response function, employing the Herman–Kluk frozen Gaussian approximation to the quantum propagator in the coherent states representation. This semiclassical approximation permits the response function to be computed from classical trajectories and stability matrices, and provides insight into the relationship between nonlinear response in classical and quantum mechanics. Linear response calculations for an anharmonic oscillator illustrate that the semiclassical approach reproduces the significant differences between quantum and classical results. © *2003 American Institute of Physics.* [DOI: 10.1063/1.1577319]

I. INTRODUCTION

Coherent multiple pulse infrared spectroscopies have the capacity to provide a picture of nuclear dynamics in the ground electronic state of a complex condensed-phase molecular system that is unobtainable from a conventional absorption spectrum.[1] Members of this family of measurements have been applied to a variety of liquid phase systems, including biomolecules.[2–9] Modeling the observables in such experiments rigorously at the atomic level requires performing quantum dynamical simulations for large anharmonic systems, a task that remains a severe challenge.

The difficulty of quantum mechanical calculations of the nonlinear vibrational response functions[10] probed in these measurements provides a strong motivation for investigating the validity of classical mechanical or semiclassical approaches to these observables. Mukamel *et al.*[11] have presented a classical mechanical formulation of nonlinear optical response theory, showing that classical calculation of nonlinear optical response functions requires evaluating stability matrices and higher order stability derivatives, depending on the order of the response function and the form of the radiation–matter interaction. Thus, a conventional molecular dynamics simulation that computes only trajectories does not suffice to evaluate classical nonlinear optical response functions. Loring and co-workers have assessed the validity of the classical computation of the two-pulse vibrational echo for a model of an anharmonic oscillator coupled to a harmonic solvent.[12–16] Their work demonstrates that for the case of a single degree of freedom coupled to radiation and interacting nonresonantly with other degrees of freedom of lower frequency, a completely classical calculation is at least qualitatively correct and can be quantitatively accurate. This scenario approximately describes the case of infrared echo measurements on the CO vibration in carbonmonoxymyoglobin by Fayer and co-workers.[2–4]

The use of semiclassical approximations to quantum propagators provides a promising strategy for introducing aspects of quantum dynamics into the motions of systems near the classical limit.[17–30] In addition to requiring the computation of classical trajectories, calculations employing these propagators typically involve the determination of classical stability matrices,[23,31] which provide approximate contributions to the dynamics from nonclassical paths in the vicinity of the classical trajectory. However, classical computations of nonlinear response functions also require the evaluation of stability derivatives, for a different physical reason. The requirement of both trajectory and stability matrix calculations[11] as input to a purely classical determination of a nonlinear response function provides motivation to develop semiclassical algorithms in which the same level of information can provide an approximate treatment of quantum dynamics. In addition, purely classical calculations of vibrational echoes[15,16] suggest that the classical description can be a reasonable zeroth order picture, implying that quantum effects could be successfully incorporated through a semiclassical approach.

Early applications[19,20] of semiclassical methods to problems of chemical dynamics exploited the Van Vleck approximation[17,18,23] to the quantum mechanical propagator. Although the Van Vleck propagator provides an approximation to the full quantum propagator that requires only classical mechanical quantities as input [see Eq. (A1) below], its direct use presents several difficulties. First, it is necessary to solve the double-ended boundary value or root search problem associated with the determination of a classical trajectory (or, in general, several or no trajectories) connecting two given points in coordinate space in a fixed time. Second, the prefactor in the Van Vleck propagator can exhibit divergences associated with the existence of conjugate points; these divergences are analogous to the singular behavior of primitive WKB wave functions at turning points.[18] Third, it is necessary to keep track of the Morse–Maslov index, which is a phase factor associated with the passage of classical trajectories through conjugate points.[23,32]

Despite some recent progress in the direct solution of the double-ended boundary value problem for classical trajectories,[33,34] most recent applications of semiclassical mechanics have exploited the initial value representation (IVR)[35,36] of the propagator.[21,22,25,27–30,37–40] Using the IVR, it is possible to propagate trajectories specified by an initial coordinate-momentum pair, rather than initial and final coordinate values. The Herman–Kluk (HK) representation of the propagator in particular has been widely applied.[21,22,28,29] The HK propagator is a frozen-Gaussian[41] IVR approximation to the propagator in the coherent state representation.[26,42,43] Alternatives to the original derivation of this propagator by Herman and Kluk[21] have recently been given by Grossmann and Xavier[44] and by Miller.[45,46] Kay has discussed general integral representations of the semiclassical propagator.[38] In addition to providing a semiclassical IVR for the propagator, the HK approximation has the useful property that the prefactor [see Eq. (5) below] is always well-behaved with magnitude never zero or divergent. The appropriate phase of the prefactor (branch of the square root function) is therefore easily determined through continuity.[38,40]

Herman and Coker[47] have considered the physical interpretation of the approach to the classical limit of observables in many-body, classically chaotic systems, as computed with the HK approximation to the quantum propagator. In the context of the calculation of an equilibrium or nonequilibrium correlation function of two quantum operators, their analysis shows that the classical limit is approached through interference between the two propagators associated with the bra and ket ''sides'' of the density operator.[10] Hence the classical limit is not obviously manifest at the amplitude level, as wave functions will in general exhibit delocalization. The classical limit of quantum correlation functions has been considered from a similar perspective by Voth and co-workers,[48,49] Sun and Miller,[50] Makri and co-workers[51–53] and McWhirter.[54]

In the present work, we consider the semiclassical calculation of optical response functions with the HK propagator. Nonlinear response functions have the form of equilibrium averages of nested commutators involving the operator governing the radiation–matter interaction. The nth order response function can be written as a sum of 2^n correlation functions, and the analysis of Herman and Coker can, in principle, be applied to each of these. Here, we develop a compact semiclassical expression for the general nth order response function, which does not involve expansion as a sum of correlation functions, and analyze the approach to the classical limit. This analysis represents a generalization of the treatment of Herman and Coker[47] of a two-time correlation function to a nonlinear response function of any order. As a first example of the numerical application of this strategy, we present semiclassical calculations of the linear response of a Morse oscillator,[55] which are compared to exact classical and quantum results. The semiclassical calculation is shown to compare well with the quantum result over a range of temperatures and numbers of bound states of the oscillator, suggesting promise for future calculations of the nonlinear response of anharmonic systems.

The semiclassical formalism for the nonlinear response function using the HK propagator is developed in Sec. II. The approach to the classical limit is considered there, as is the demonstration that the formalism is exactly correct for a harmonic system. Numerical results for the linear response of a Morse oscillator are presented and discussed in Sec. III. Our conclusions are given in Sec. IV. Appendix A presents an alternative semiclassical form for nonlinear response functions based on the coordinate-space Van Vleck propagator.[17] The approach to the classical limit in this formulation is discussed there, and the structure of the coordinate-space result is compared to the semiclassical response function computed with coherent states derived in Sec. II. Certain technical points are reserved for Appendices B and C. An identity [shown in Eq. (26)] employed in the analysis of the harmonic limit of the response functions is derived in Appendix B, where an alternative formalism for the semiclassical response functions in terms of complexified coherent states is also discussed. A second identity [shown in Eq. (27)] required in extracting the classical limit of the semiclassical response function, is justified in Appendix C. This appendix restates the identity proven in the Appendix of the paper by Herman and Coker[47] in our notation, with particular emphasis given to the symplectic nature of the stability matrix.[23,31]

II. SEMICLASSICAL RESPONSE FUNCTIONS

The classical mechanical electric polarization generated in a material by an electric field $E(t)$ to nth order in perturbation theory in the field-material interaction, $P^{(n)}(t)$, is controlled by the response function $R^{(n)}$,

$$P^{(n)}(t)=\int_0^\infty dt_n\cdots\int_0^\infty dt_1 R^{(n)}(t_n,\ldots,t_1)\times E(t-t_n)\cdots E(t-t_1-\cdots t_n). \tag{1}$$

The time variable t_j denotes the elapsed time between successive material–field interactions. Relevant material dynamics are assumed to involve length scales small compared to the wavelength of the applied radiation, so that the spatial dependences of quantities in Eq. (1) can be neglected. We specialize to a system with F degrees of freedom, one of which is coupled to the field through an electric dipole interaction. The electric dipole of this ''active'' degree of freedom is taken to be proportional to its coordinate. In this case, the response function[10] takes the form,

$$R^{(n)}(t_n,\ldots,t_1)=\left(\frac{i}{\hbar}\right)^n \mathrm{Tr}\{\hat{x}\hat{K}(t_n)[\hat{x},\hat{K}(t_{n-1})[\hat{x},\ldots[\hat{x},\hat{K}(t_1)\times[\hat{x},\hat{\rho}]\hat{K}^\dagger(t_1)]\cdots]\hat{K}^\dagger(t_{n-1})]\hat{K}^\dagger(t_n)\}. \tag{2}$$

The coordinate of the active degree of freedom is denoted $\hat{x}$, $\hat{K}(t)\equiv\exp(-i\hat{H}t/\hbar)$ represents the quantum mechanical

propagator associated with the Hamiltonian $\hat{H}$ for all F degrees of freedom, and $\hat{\rho}$ is the equilibrium density matrix. The proportionality constant relating $\hat{x}$ to the dipole operator is suppressed.

Semiclassical expressions for the response function of Eq. (2) may be obtained by replacing the quantum mechanical propagator $\hat{K}(t)$ with a semiclassical approximation. Although the detailed form of the semiclassical approximation to $R^{(n)}$ differs according to the choice of semiclassical propagator, the resulting expressions share a common structure involving propagation of pairs of classical trajectories for times t_k, with ''jumps'' (either in momentum or in phase space) occurring between trajectory segments.

One possible choice is to evaluate the trace in Eq. (2) in the coordinate representation and use the Van Vleck propagator.[17,18,23] This case is discussed in some detail in Appendix A. The results obtained in Appendix A using the Van Vleck propagator are of considerable interest for the insights they provide into the structure of the semiclassical response function, and in particular the passage to the classical limit. However, computational implementation of the expressions derived, which are of the type denoted SC IVR by Miller,[29] is not entirely straightforward. As mentioned in the Introduction, it is necessary to keep track of the Morse–Maslov phase for each classical trajectory segment.

Another possibility is to use the HK propagator,[21,22,28,29] which is a semiclassical approximation in the coherent state representation. Use of the HK propagator has the advantage that explicit determination of a Morse–Maslov phase is not necessary.[38,40] The HK propagator has been widely applied to problems in chemical dynamics,[28,29] and is the focus of the present work.

The Herman–Kluk propagator has the form,[21,22]

$$\hat{K}(t) \rightarrow (2\pi\hbar)^{-F} \int d\mathbf{z} |\mathbf{z}(t)\rangle G(\mathbf{z},t) \langle \mathbf{z}|, \tag{3}$$

with

$$G(\mathbf{z},t) = C(\mathbf{z},t) \exp[iS(\mathbf{z},t)/\hbar], \tag{4}$$

$$C(\mathbf{z},t) = \sqrt{\det \frac{1}{2}\left[\mathbf{M}_{qq}(\mathbf{z},t) + \mathbf{M}_{pp}(\mathbf{z},t) - i\hbar\gamma \mathbf{M}_{qp}(\mathbf{z},t) + \frac{i}{\hbar\gamma} \mathbf{M}_{pq}(\mathbf{z},t) \right]}. \tag{5}$$

In Eq. (3), $\mathbf{z}$ represents a point in $2F$-dimensional phase space, $\mathbf{z}(t)$ represents the phase space point that results from propagating a classical trajectory of duration t from $\mathbf{z}$, and $|\mathbf{z}\rangle$ denotes a coherent state, characterized by F-dimensional coordinate and momentum $\mathbf{q}$ and $\mathbf{p}$, and spatial width parameter γ, whose coordinate-space wave function is given by

$$\langle \mathbf{r}|\mathbf{z}\rangle = \left(\frac{\gamma}{\pi}\right)^{F/4} \exp\left[-\frac{\gamma}{2}(\mathbf{r}-\mathbf{q})^2 + \frac{i}{\hbar}\mathbf{p}\cdot(\mathbf{r}-\mathbf{q}) \right]. \tag{6}$$

The classical action (Hamilton's principal function) associated with the trajectory of duration t starting at $\mathbf{z}$ is denoted $S(\mathbf{z},t)$. Equation (5) contains F-dimensional stability matrices associated with the trajectory of duration t beginning at phase point $\mathbf{z}$, with elements given by, for example,

$$[\mathbf{M}_{qp}]_{\alpha\beta} \equiv \left(\frac{\partial q_\alpha(t)}{\partial p_\beta(0)} \right)_{\{p_\nu(0)\}_{\nu\neq\beta}\{q_\nu(0)\}}, \tag{7}$$

with α, β, and ν labelling degrees of freedom. The active degree of freedom will be designated $\alpha = 0$.

In principle, $R^{(n)}$ can be evaluated by expanding the nested commutators in Eq. (2) to produce a sum of 2^n equilibrium correlation functions of the coordinate operator at $n+1$ times.[10] However, a more compact form is more likely to be suitable for numerical evaluation. Substitution of the HK propagator into Eq. (2) will generate matrix elements between coherent states of commutators of $\hat{x}$ with other operators. The following identity, which may be verified by explicit evaluation in the coordinate representation, provides a useful form for such matrix elements;

$$\langle \mathbf{z}_1|[\hat{x},\hat{A}]|\mathbf{z}_2\rangle = i\hbar\langle \mathbf{z}_1|\mathbf{z}_2\rangle \frac{\partial}{\partial \overline{p}_{12}} \left(\frac{\langle \mathbf{z}_1|\hat{A}|\mathbf{z}_2\rangle}{\langle \mathbf{z}_1|\mathbf{z}_2\rangle} \right), \tag{8}$$

$$\overline{p}_{12} = [(\mathbf{p}_1)_0 + (\mathbf{p}_2)_0]/2. \tag{9}$$

$\hat{A}$ represents any operator, and $\overline{p}_{12}$ is the mean momentum for the active degree of freedom at the two phase points $\mathbf{z}_1$ and $\mathbf{z}_2$. The partial derivative in Eq. (8) is taken at fixed values of $(\mathbf{q}_1)_\alpha$ and $(\mathbf{q}_2)_\alpha$, at fixed values of $(\mathbf{p}_1)_\alpha$ and $(\mathbf{p}_2)_\alpha$ with $\alpha > 0$, and at fixed value of $\Delta p_{12} \equiv (\mathbf{p}_1)_0 - (\mathbf{p}_2)_0$.

Application of the identity in Eq. (8) and the HK approximation in Eq. (3) permits the response function in Eq. (2) to be written in a relatively compact form,

$$R^{(n)}(t_n,\ldots,t_1)=(-1)^n\int\frac{d\mathbf{z}_1}{(2\pi\hbar)^F}\int\frac{d\mathbf{z}_2}{(2\pi\hbar)^F}\cdots\int\frac{d\mathbf{z}_{2n}}{(2\pi\hbar)^F}G(\mathbf{z}_1,t_1)G^*(\mathbf{z}_2,t_1)\cdots G(\mathbf{z}_{2n-1},t_n)G^*(\mathbf{z}_{2n},t_n)$$
$$\times\left\{\langle\mathbf{z}_{2n}(t_n)|\mathbf{z}_{2n-1}(t_n)\rangle\left[\overline{q}_{2n-1,2n}(t_n)+\frac{i}{2\hbar\gamma}\Delta p_{2n-1,2n}(t_n)\right]\right\}$$
$$\times\left\{\langle\mathbf{z}_{2n-1}|\mathbf{z}_{2n}\rangle\left[\frac{\partial}{\partial\overline{p}_{2n-1,2n}}\left(\frac{\langle\mathbf{z}_{2n-2}(t_{n-1})|\mathbf{z}_{2n}\rangle\langle\mathbf{z}_{2n-1}|\mathbf{z}_{2n-3}(t_{n-1})\rangle}{\langle\mathbf{z}_{2n-1}|\mathbf{z}_{2n}\rangle}\right)\right]\right\}$$
$$\times\left\{\langle\mathbf{z}_{2n-3}|\mathbf{z}_{2n-2}\rangle\left[\frac{\partial}{\partial\overline{p}_{2n-3,2n-2}}\left(\frac{\langle\mathbf{z}_{2n-4}(t_{n-2})|\mathbf{z}_{2n-2}\rangle\langle\mathbf{z}_{2n-3}|\mathbf{z}_{2n-5}(t_{n-2})\rangle}{\langle\mathbf{z}_{2n-3}|\mathbf{z}_{2n-2}\rangle}\right)\right]\right\}\cdots$$
$$\times\left\{\langle\mathbf{z}_3|\mathbf{z}_4\rangle\left[\frac{\partial}{\partial\overline{p}_{34}}\left(\frac{\langle\mathbf{z}_2(t_1)|\mathbf{z}_4\rangle\langle\mathbf{z}_3|\mathbf{z}_1(t_1)\rangle}{\langle\mathbf{z}_3|\mathbf{z}_4\rangle}\right)\right]\right\}\langle\mathbf{z}_1|\mathbf{z}_2\rangle\frac{\partial}{\partial\overline{p}_{12}}\left(\frac{\langle\mathbf{z}_1|\hat{\rho}|\mathbf{z}_2\rangle}{\langle\mathbf{z}_1|\mathbf{z}_2\rangle}\right). \tag{10}$$

The momentum derivatives in Eq. (10) can be performed explicitly, according to

$$\frac{\partial}{\partial\overline{p}_{ij}}\ln\left(\frac{\langle\mathbf{z}_a|\mathbf{z}_i\rangle\langle\mathbf{z}_j|\mathbf{z}_b\rangle}{\langle\mathbf{z}_j|\mathbf{z}_i\rangle}\right)=\frac{1}{i\hbar}[\mathcal{X}(\mathbf{z}_j,\mathbf{z}_b)-\mathcal{X}^*(\mathbf{z}_i,\mathbf{z}_a)], \tag{11}$$

$$\mathcal{X}(\mathbf{z}_j,\mathbf{z}_k)\equiv\frac{\langle\mathbf{z}_j|\hat{x}|\mathbf{z}_k\rangle}{\langle\mathbf{z}_j|\mathbf{z}_k\rangle}=\overline{q}_{jk}-i\frac{\Delta p_{jk}}{2\gamma\hbar}, \tag{12}$$

$$\Delta p_{jk}=(\mathbf{p}_j)_0-(\mathbf{p}_k)_0;\quad\overline{q}_{jk}=[(\mathbf{q}_j)_0+(\mathbf{q}_k)_0]/2, \tag{13}$$

to yield the following:

$$R^{(n)}(t_n,\ldots,t_1)=-\left(\frac{i}{\hbar}\right)^{n-1}\int\frac{d\mathbf{z}_1}{(2\pi\hbar)^F}\int\frac{d\mathbf{z}_2}{(2\pi\hbar)^F}\cdots\int\frac{d\mathbf{z}_{2n}}{(2\pi\hbar)^F}G(\mathbf{z}_1,t_1)G^*(\mathbf{z}_2,t_1)\cdots G(\mathbf{z}_{2n-1},t_n)$$
$$\times G^*(\mathbf{z}_{2n},t_n)\langle\mathbf{z}_{2n}(t_n)|\mathbf{z}_{2n-1}(t_n)\rangle\mathcal{X}(\mathbf{z}_{2n}(t_n),\mathbf{z}_{2n-1}(t_n))\langle\mathbf{z}_{2n-2}(t_{n-1})|\mathbf{z}_{2n}\rangle$$
$$\times\langle\mathbf{z}_{2n-1}|\mathbf{z}_{2n-3}(t_{n-1})\rangle[\mathcal{X}(\mathbf{z}_{2n-1},\mathbf{z}_{2n-3}(t_{n-1}))-\mathcal{X}^*(\mathbf{z}_{2n},\mathbf{z}_{2n-2}(t_{n-1}))]\cdots$$
$$\times\langle\mathbf{z}_2(t_1)|\mathbf{z}_4\rangle\langle\mathbf{z}_3|\mathbf{z}_1(t_1)\rangle[\mathcal{X}(\mathbf{z}_3,\mathbf{z}_1(t_1))-\mathcal{X}^*(\mathbf{z}_4,\mathbf{z}_2(t_1))]\langle\mathbf{z}_1|\mathbf{z}_2\rangle\frac{\partial}{\partial\overline{p}_{12}}\left(\frac{\langle\mathbf{z}_1|\hat{\rho}|\mathbf{z}_2\rangle}{\langle\mathbf{z}_1|\mathbf{z}_2\rangle}\right). \tag{14}$$

This expression contains no approximations other than the HK approximation to the propagator. Its evaluation requires calculating the matrix element between coherent states of the equilibrium density matrix and propagating n pairs of classical trajectories of duration t_1, t_2,..., t_n from initial phase points $\mathbf{z}_1,\ldots,\mathbf{z}_{2n}$. The expression in Eq. (14) shows its origin in the n nested commutators with the coordinate operator of Eq. (2). Expanding the $n-1$ products of differences of $\mathcal{X}$ functions yields 2^{n-1} distinct terms that contribute to $R^{(n)}$. There are 2^{n-1} rather than 2^n terms[10] because we retain the momentum derivative of the expression involving the density operator.

The structure of the semiclassical approximation to $R^{(n)}$ in Eq. (14) may be represented with the diagram shown in Fig. 1. Filled vertices represent phase points to be integrated over, and open vertices represent phase points that have been propagated for one of the time intervals. Each upward-pointing solid arrow represents a classical trajectory and carries a factor of $G(\mathbf{z},t)$ on the left-hand side of the diagram, and $G^*(\mathbf{z},t)$ on the right-hand side of the diagram. The lower horizontal line connecting filled vertices signifying phase points $\mathbf{z}_1$ and $\mathbf{z}_2$ represents the factor $-\langle\mathbf{z}_1|\mathbf{z}_2\rangle\partial(\langle\mathbf{z}_1|\hat{\rho}|\mathbf{z}_2\rangle/\langle\mathbf{z}_1|\mathbf{z}_2\rangle)/\partial\overline{p}_{12}$, and the upper horizontal line connecting open vertices signifying phase points $\mathbf{z}_{2n-1}(t_n)$ and $\mathbf{z}_{2n}(t_n)$ represents the factor $\langle\mathbf{z}_{2n}(t_n)|\hat{x}|\mathbf{z}_{2n-1}(t_n)\rangle$. A dashed horizontal line connecting vertices for $\mathbf{z}_{2j-1}$ and $\mathbf{z}_{2j}$ represents the factor $i[\mathcal{X}(\mathbf{z}_{2j-1},\mathbf{z}_{2j-3}(t_{j-1}))-\mathcal{X}^*(\mathbf{z}_{2j},\mathbf{z}_{2j-2}(t_{j-1}))]/\hbar$. A vertical dotted line connecting vertices for $\mathbf{z}_{2j-3}(t_{j-1})$ and $\mathbf{z}_{2j-1}$ on the left-hand side of the diagram represents the factor $\langle\mathbf{z}_{2j-3}(t_{j-1})|\mathbf{z}_{2j-1}\rangle^*$, and a vertical dotted line connecting vertices for $\mathbf{z}_{2j-2}(t_{j-1})$ and $\mathbf{z}_{2j}$ on the right-hand side of the diagram represents the factor $\langle\mathbf{z}_{2j-2}(t_{j-1})|\mathbf{z}_{2j}\rangle$. This diagrammatic representation emphasizes the contribution of $2n$ distinct trajectory segments to the integrand of $R^{(n)}$.

Insight into the structure of this semiclassical expression for the response function may be gained by verifying that it is exactly correct for a harmonic system, and also embodies the correct classical mechanical limit for an anharmonic potential. We begin by considering these limits in the special case of the linear response, $n=1$, and then generalize the arguments to the nonlinear response of any order. Setting $n=1$ in Eq. (10) or Eq. (14) gives the linear response function within the HK approximation to the propagator,

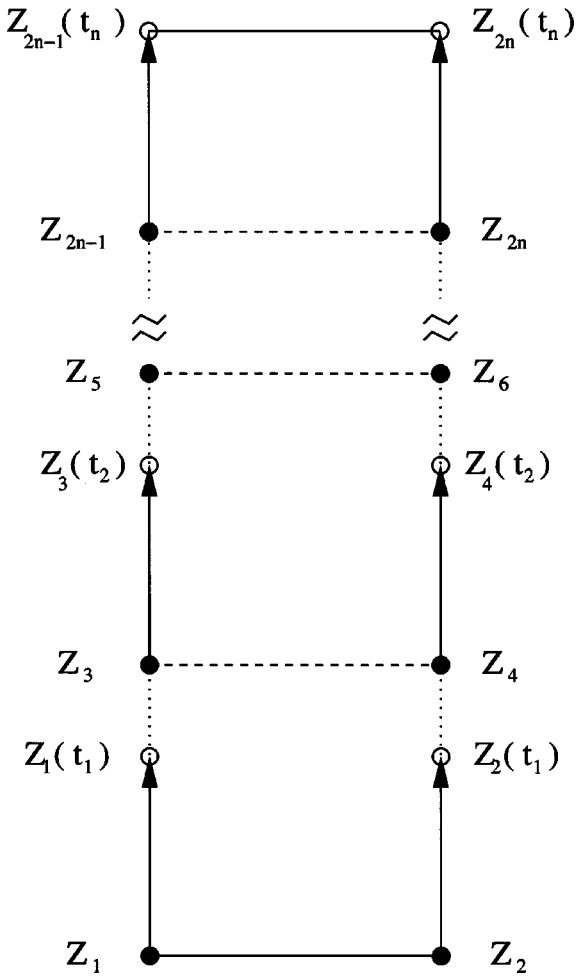

FIG. 1. The nth order nonlinear optical response function, evaluated with the semiclassical Herman–Kluk propagator and shown in Eq. (14), is represented as a diagram.

$$R^{(1)}(t)=-\int\frac{d\mathbf{z}_1}{(2\pi\hbar)^F}\int\frac{d\mathbf{z}_2}{(2\pi\hbar)^F}G(\mathbf{z}_1,t)G^*(\mathbf{z}_2,t)\times\langle\mathbf{z}_2(t)|\mathbf{z}_1(t)\rangle\langle\mathbf{z}_1|\mathbf{z}_2\rangle\left[\overline{q}_{12}(t)+\frac{i}{2\hbar\gamma}\Delta p_{12}(t)\right]\times\frac{\partial}{\partial\overline{p}_{12}}\left(\frac{\langle\mathbf{z}_1|\hat{\rho}|\mathbf{z}_2\rangle}{\langle\mathbf{z}_1|\mathbf{z}_2\rangle}\right). \tag{15}$$

Evaluation of this integrand requires propagating two trajectories of duration t, starting at phase points $\mathbf{z}_1$ and $\mathbf{z}_2$. The

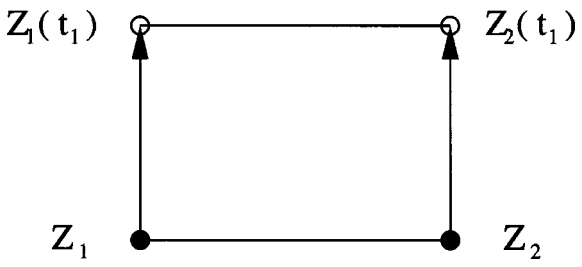

FIG. 2. The semiclassical linear response function shown in Eq. (15) is represented as a diagram.

tories of duration t, starting at phase points $\mathbf{z}_1$ and $\mathbf{z}_2$. The diagram representing $R^{(1)}$, a special case of the diagram in Fig. 1, is shown in Fig. 2.

We expect that in the classical limit, the dominant contributions to the integral in Eq. (15) will involve trajectories with initial conditions $\mathbf{z}_1$ and $\mathbf{z}_2$ that are nearby in phase space. We therefore expand the logarithm of the product $G(\mathbf{z}_1,t)G^*(\mathbf{z}_2,t)$ about the mean phase point, $\overline{\mathbf{z}}_{12}$,

$$G(\mathbf{z}_1,t)G^*(\mathbf{z}_2,t)\rightarrow|C(\overline{\mathbf{z}}_{12},t)|^2\exp\left[\frac{i}{\hbar}((\overline{\mathbf{p}}_{12}(t)\cdot\mathbf{M}_{qq}(\overline{\mathbf{z}}_{12},t)-\overline{\mathbf{p}}_{12})\cdot\Delta\mathbf{q}_{12}+\overline{\mathbf{p}}_{12}(t)\cdot\mathbf{M}_{qp}(\overline{\mathbf{z}}_{12},t)\cdot\Delta\mathbf{p}_{12})\right], \tag{16}$$

with

$$\overline{\mathbf{y}}_{12}=(\mathbf{y}_1+\mathbf{y}_2)/2,\quad\Delta\mathbf{y}_{12}=\mathbf{y}_1-\mathbf{y}_2;\quad\mathbf{y}=\mathbf{q},\mathbf{p}. \tag{17}$$

This expression was obtained by replacing the HK prefactors in Eq. (5) at phase points $\mathbf{z}_1$ and $\mathbf{z}_2$ with the prefactor for the mean phase point $\overline{\mathbf{z}}_{12}$, and expanding the difference of actions, $S(\mathbf{z}_1,t)-S(\mathbf{z}_2,t)$ to second order in deviations of the initial phase points from $\overline{\mathbf{z}}_{12}$. The manipulation in Eq. (16) is also exactly correct for a harmonic system. In Eq. (15), the product $G(\mathbf{z}_1,t)G^*(\mathbf{z}_2,t)$ is multiplied by the coherent states overlaps $\langle\mathbf{z}_2(t)|\mathbf{z}_1(t)\rangle\langle\mathbf{z}_1|\mathbf{z}_2\rangle$, with

$$\langle\mathbf{z}_2(t)|\mathbf{z}_1(t)\rangle=\exp\left[-\frac{\gamma}{4}(\Delta\mathbf{q}_{12}(t))^2\right]\times\exp\left[-\frac{1}{4\gamma\hbar^2}(\Delta\mathbf{p}_{12}(t))^2\right]\times\exp\left[-\frac{i}{\hbar}\overline{\mathbf{p}}_{12}(t)\cdot\Delta\mathbf{q}_{12}(t)\right]. \tag{18}$$

In keeping with our assumption of nearby initial phase points, we linearize the time-dependent difference coordinates and momenta in Eq. (18),

$$\Delta\mathbf{q}_{12}(t)\rightarrow\mathbf{M}_{qq}(\overline{\mathbf{z}}_{12},t)\cdot\Delta\mathbf{q}_{12}+\mathbf{M}_{qp}(\overline{\mathbf{z}}_{12},t)\cdot\Delta\mathbf{p}_{12},$$
$$\Delta\mathbf{p}_{12}(t)\rightarrow\mathbf{M}_{pq}(\overline{\mathbf{z}}_{12},t)\cdot\Delta\mathbf{q}_{12}+\mathbf{M}_{pp}(\overline{\mathbf{z}}_{12},t)\cdot\Delta\mathbf{p}_{12}. \tag{19}$$

Within this approximation, the product of the phase factors from $G(\mathbf{z}_1,t)G^*(\mathbf{z}_2,t)\langle\mathbf{z}_2(t)|\mathbf{z}_1(t)\rangle\langle\mathbf{z}_1|\mathbf{z}_2\rangle$ is unity, and this product takes the real-valued Gaussian form,

$$[G(\mathbf{z}_1,t)G^*(\mathbf{z}_2,t)\langle\mathbf{z}_2(t)|\mathbf{z}_1(t)\rangle\langle\mathbf{z}_1|\mathbf{z}_2\rangle]_{\mathrm{lin}}=|C(\overline{\mathbf{z}}_{12},t)|^2\exp\left[-\frac{1}{4}\Delta\mathbf{Z}_{12}^T\cdot[\mathbf{I}_{2F}+\overline{\mathbf{M}}^T\cdot\overline{\mathbf{M}}]\cdot\Delta\mathbf{Z}_{12}\right], \tag{20}$$

with

$$\overline{\mathbf{M}}=\begin{bmatrix}\mathbf{M}_{qq}(\overline{\mathbf{z}}_{12},t) & \hbar\gamma\mathbf{M}_{qp}(\overline{\mathbf{z}}_{12},t)\\ (\hbar\gamma)^{-1}\mathbf{M}_{pq}(\overline{\mathbf{z}}_{12},t) & \mathbf{M}_{pp}(\overline{\mathbf{z}}_{12},t)\end{bmatrix}, \tag{21}$$

$$\Delta\mathbf{Z}=\begin{bmatrix}\sqrt{\gamma}\Delta\mathbf{q}_{12}\\ (\hbar\sqrt{\gamma})^{-1}\Delta\mathbf{p}_{12}\end{bmatrix}. \tag{22}$$

The subscript lin in Eq. (20) indicates the linearization approximation of Eqs. (16) and (19). The expression in Eq. (20) is exactly correct for a harmonic system.

Changing integration variables in Eq. (15) from $\mathbf{z}_1$ and $\mathbf{z}_2$ to $\overline{\mathbf{z}}_{12}$ and $\Delta\mathbf{z}_{12}$, integrating once by parts with respect to $\overline{p}_{12}$, and linearizing the integrand as in Eqs. (19) and (20) yields the following for $R^{(1)}(t)$:

$$R^{(1)}(t)=\int\frac{d\Delta\mathbf{z}_{12}}{(2\pi\hbar)^F}\int\frac{d\overline{\mathbf{z}}_{12}}{(2\pi\hbar)^F}\frac{\partial}{\partial\overline{p}_{12}}\times\left\{[G(\mathbf{z}_1,t)G^*(\mathbf{z}_2,t)\langle\mathbf{z}_2(t)|\mathbf{z}_1(t)\rangle\langle\mathbf{z}_1|\mathbf{z}_2\rangle]_{\mathrm{lin}}\times\left[\overline{q}_{12}(t)+\frac{i}{2\hbar\gamma}(\Delta p_{12}(t))_{\mathrm{lin}}\right]\right\}\frac{\langle\mathbf{z}_1|\hat{\rho}|\mathbf{z}_2\rangle}{\langle\mathbf{z}_1|\mathbf{z}_2\rangle}. \tag{23}$$

The integrand in Eq. (23) contains a partial derivative with respect to $\overline{p}_{12}$ of a product of two factors, whose dependence on this quantity we now examine. According to Eq. (20), the quantity $[G(\mathbf{z}_1,t)G^*(\mathbf{z}_2,t)\langle\mathbf{z}_2(t)|\mathbf{z}_1(t)\rangle\langle\mathbf{z}_1|\mathbf{z}_2\rangle]_{\mathrm{lin}}$ depends on $\overline{p}_{12}$ only through stability matrices, and hence is independent of $\overline{p}_{12}$ for a harmonic system, in which stability matrices are independent of initial conditions. The factor $(\Delta p_{12}(t))_{\mathrm{lin}}$ is independent of $\overline{p}_{12}$ at fixed Δp_{12}. For a harmonic system, the momentum derivative in Eq. (23) acts only on the factor $\overline{q}_{12}(t)$. To obtain the correct classical limit for an anharmonic system, we will neglect the derivatives[27,45] with respect to $\overline{p}_{12}$ of the stability matrices in Eq. (20). The linear response function is then given by

$$R^{(1)}(t)=\int\frac{d\overline{\mathbf{z}}_{12}}{(2\pi\hbar)^F}\frac{\partial\overline{q}_{12}(t)}{\partial\overline{p}_{12}}\int\frac{d\Delta\mathbf{z}_{12}}{(2\pi\hbar)^F}\frac{\langle\mathbf{z}_1|\hat{\rho}|\mathbf{z}_2\rangle}{\langle\mathbf{z}_1|\mathbf{z}_2\rangle}\times[G(\mathbf{z}_1,t)G^*(\mathbf{z}_2,t)\langle\mathbf{z}_2(t)|\mathbf{z}_1(t)\rangle\langle\mathbf{z}_1|\mathbf{z}_2\rangle]_{\mathrm{lin}}. \tag{24}$$

The expression in Eq. (24) may be used both to demonstrate the exactly correct result for a harmonic system, and the correct classical limit for a general potential.

In the harmonic case, the stability derivative $\partial\overline{q}_{12}(t)/\partial\overline{p}_{12}\equiv\partial(\mathbf{q}(t))_0/\partial(\mathbf{p})_0$ is independent of $\overline{\mathbf{z}}_{12}$, so that

$$R^{(1)}(t)=\frac{\partial(\mathbf{q}(t))_0}{\partial(\mathbf{p})_0}\int\frac{d\Delta\mathbf{z}_{12}}{(2\pi\hbar)^F}[G(\mathbf{z}_1,t)G^*(\mathbf{z}_2,t)\times\langle\mathbf{z}_2(t)|\mathbf{z}_1(t)\rangle\langle\mathbf{z}_1|\mathbf{z}_2\rangle]_{\mathrm{lin}}\int\frac{d\overline{\mathbf{z}}_{12}}{(2\pi\hbar)^F}\frac{\langle\mathbf{z}_1|\hat{\rho}|\mathbf{z}_2\rangle}{\langle\mathbf{z}_1|\mathbf{z}_2\rangle}. \tag{25}$$

It must be emphasized that while the factor $[G(\mathbf{z}_1,t)G^*(\mathbf{z}_2,t)\langle\mathbf{z}_2(t)|\mathbf{z}_1(t)\rangle\langle\mathbf{z}_1|\mathbf{z}_2\rangle]_{\mathrm{lin}}$ is independent of $\overline{\mathbf{z}}_{12}$ for a harmonic system, the factor $\langle\mathbf{z}_1|\hat{\rho}|\mathbf{z}_2\rangle/\langle\mathbf{z}_1|\mathbf{z}_2\rangle$ depends on both $\overline{\mathbf{z}}_{12}$ and $\Delta\mathbf{z}_{12}$. According to an identity demonstrated in Appendix B, the integral over $\overline{\mathbf{z}}_{12}$ in Eq. (25) is unity for any normalized density matrix,

$$\int\frac{d\overline{\mathbf{z}}_{12}}{(2\pi\hbar)^F}\frac{\langle\mathbf{z}_1|\hat{\rho}|\mathbf{z}_2\rangle}{\langle\mathbf{z}_1|\mathbf{z}_2\rangle}=1. \tag{26}$$

A second identity,[47,56] verified in Appendix C, holds for both harmonic and anharmonic potentials,

$$\int\frac{d\Delta\mathbf{z}_{12}}{(2\pi\hbar)^F}[G(\mathbf{z}_1,t)G^*(\mathbf{z}_2,t)\langle\mathbf{z}_2(t)|\mathbf{z}_1(t)\rangle\langle\mathbf{z}_1|\mathbf{z}_2\rangle]_{\mathrm{lin}}=1. \tag{27}$$

Performing the integrations in Eq. (25) with Eqs. (26) and (27) gives the exactly correct linear response function for a harmonic system, $R^{(1)}(t)=\partial(\mathbf{q}(t))_0/\partial(\mathbf{p})_0$, independent of $\hbar$ and properties of the initial distribution such as temperature.

We return to Eq. (24) to extract the correct classical mechanical limit of $R^{(1)}(t)$ for an anharmonic potential. This limit may be achieved by the substitution

$$\frac{1}{(2\pi\hbar)^F}\frac{\langle\mathbf{z}_1|\hat{\rho}|\mathbf{z}_2\rangle}{\langle\mathbf{z}_1|\mathbf{z}_2\rangle}\rightarrow f_{\mathrm{cl}}(\overline{\mathbf{z}}_{12}), \tag{28}$$

with the classical phase space distribution denoted $f_{\mathrm{cl}}(\mathbf{z})$. This high-temperature approximation to the matrix element of the density operator between coherent states is similar to the high-temperature approximation discussed by Herman and Coker[47] with the additional approximation that the average potential in their expression, $[V(\mathbf{q}_1)+V(\mathbf{q}_2)]/2$, is replaced by the potential at the average coordinate, $V(\overline{\mathbf{q}}_{12})$. Within this approximation, the integration over $\Delta\mathbf{z}_{12}$ in Eq. (24) may be performed using the identity in Eq. (27) to give the correct classical mechanical expression for the linear response function,

$$R^{(1)}(t)=\int d\overline{\mathbf{z}}_{12}\frac{\partial\overline{q}_{12}(t)}{\partial\overline{p}_{12}}f_{\mathrm{cl}}(\overline{\mathbf{z}}_{12}). \tag{29}$$

This analysis illustrates a route to the classical limit of the semiclassical linear response function for arbitrary potential. The structure of $R^{(n)}$ for $n>1$ is more complicated than that of $R^{(1)}$, because of the presence of more than one commutator in Eq. (2). Here we present the additional steps required to verify the correct harmonic and classical limits for $R^{(n)}$ with $n>1$. We begin with the integrations over the initial conditions for the pair of trajectories of duration t_n in Eq. (10),

$$J_{2n-3,2n-2}\equiv-\int\frac{d\overline{\mathbf{z}}_{2n-1,2n}}{(2\pi\hbar)^F}\int\frac{d\Delta\mathbf{z}_{2n-1,2n}}{(2\pi\hbar)^F}[G(\mathbf{z}_{2n-1},t_n)G^*(\mathbf{z}_{2n},t_n)\langle\mathbf{z}_{2n}(t_n)|\mathbf{z}_{2n-1}(t_n)\rangle\langle\mathbf{z}_{2n-1}|\mathbf{z}_{2n}\rangle]\times\left[\overline{q}_{2n-1,2n}(t_n)+\frac{i}{2\hbar\gamma}\Delta p_{2n-1,2n}(t_n)\right]\frac{\partial}{\partial\overline{p}_{2n-1,2n}}\left(\frac{\langle\mathbf{z}_{2n-2}(t_{n-1})|\mathbf{z}_{2n}\rangle\langle\mathbf{z}_{2n-1}|\mathbf{z}_{2n-3}(t_{n-1})\rangle}{\langle\mathbf{z}_{2n-1}|\mathbf{z}_{2n}\rangle}\right). \tag{30}$$

This quantity represents the value of that section of the diagram in Fig. 1 above and including the vertices labeled $\mathbf{z}_{2n-1}$ and $\mathbf{z}_{2n}$, as well as the vertical dotted lines attached to these vertices. Making the linearization approximation discussed in connection with Eq. (23) and integrating by parts with respect to $\overline{p}_{2n-1,2n}$ produces

$$J_{2n-3,2n-2}=\int \frac{d\overline{\mathbf{z}}_{2n-1,2n}}{(2\pi\hbar)^F}\int \frac{d\Delta\mathbf{z}_{2n-1,2n}}{(2\pi\hbar)^F}[G(\mathbf{z}_{2n-1},t_n)G^*(\mathbf{z}_{2n},t_n)\langle\mathbf{z}_{2n}(t_n)|\mathbf{z}_{2n-1}(t_n)\rangle\langle\mathbf{z}_{2n-1}|\mathbf{z}_{2n}\rangle]_{\rm lin}$$
$$\times\left(\frac{\partial\overline{q}_{2n-1,2n}(t_n)}{\partial\overline{p}_{2n-1,2n}}\right)\frac{\langle\mathbf{z}_{2n-2}(t_{n-1})|\mathbf{z}_{2n}\rangle\langle\mathbf{z}_{2n-1}|\mathbf{z}_{2n-3}(t_{n-1})\rangle}{\langle\mathbf{z}_{2n-1}|\mathbf{z}_{2n}\rangle}. \tag{31}$$

To proceed towards the classical mechanical limit for $R^{(n)}$, we must make the following approximation in Eq. (31):

$$\frac{\langle\mathbf{z}_{2n-2}(t_{n-1})|\mathbf{z}_{2n}\rangle\langle\mathbf{z}_{2n-1}|\mathbf{z}_{2n-3}(t_{n-1})\rangle}{\langle\mathbf{z}_{2n-1}|\mathbf{z}_{2n}\rangle}$$
$$\rightarrow(2\pi\hbar)^F\langle\mathbf{z}_{2n-2}(t_{n-1})|\mathbf{z}_{2n-3}(t_{n-1})\rangle$$
$$\times\delta(\overline{\mathbf{z}}_{2n-1,2n}-\overline{\mathbf{z}}_{2n-3,2n-2}(t_{n-1})), \tag{32}$$

with $\delta(\mathbf{z})\equiv\delta(\mathbf{q})\delta(\mathbf{p})$ signifying the $2F$-dimensional Dirac delta function. We justify this approximation by writing the relevant combination of coherent states overlaps in Eq. (32) explicitly in terms of mean and difference momenta and coordinates,

$$\frac{\langle\mathbf{z}_a|\mathbf{z}_i\rangle\langle\mathbf{z}_j|\mathbf{z}_b\rangle}{\langle\mathbf{z}_j|\mathbf{z}_i\rangle}$$
$$=\langle\mathbf{z}_a|\mathbf{z}_b\rangle\exp\left\{-\frac{\gamma}{2}\left[\overline{\mathbf{q}}_{ij}-\overline{\mathbf{q}}_{ab}+\frac{i}{2\hbar\gamma}(\Delta\mathbf{p}_{ij}+\Delta\mathbf{p}_{ab})\right]^2\right\}$$
$$\times\exp\left\{-\frac{1}{2\gamma\hbar^2}\left[\overline{\mathbf{p}}_{ij}-\overline{\mathbf{p}}_{ab}-\frac{i\gamma\hbar}{2}(\Delta\mathbf{q}_{ij}+\Delta\mathbf{q}_{ab})\right]^2\right\}. \tag{33}$$

The Gaussian factors multiplying $\langle\mathbf{z}_a|\mathbf{z}_b\rangle$ on the right-hand side of Eq. (33) are peaked about the complex values of $\overline{\mathbf{q}}_{ij}=\overline{\mathbf{q}}_{ab}-i(\Delta\mathbf{p}_{ij}+\Delta\mathbf{p}_{ab})/(2\gamma\hbar)$ and $\overline{\mathbf{p}}_{ij}=\overline{\mathbf{p}}_{ab}+i\gamma\hbar(\Delta\mathbf{q}_{ij}+\Delta\mathbf{q}_{ab})/2$. In the classical limit, the imaginary part of each vector may be neglected. The magnitudes of $\Delta\mathbf{q}_{ij}$ and $\Delta\mathbf{p}_{ij}$ are controlled by the overlap $\langle\mathbf{z}_i|\mathbf{z}_j\rangle$. Typical values of the magnitude of $\Delta\mathbf{q}_{ij}$ scale as $\gamma^{-1/2}$, and typical values of the magnitude of $\Delta\mathbf{p}_{ij}$ scale as $\hbar\gamma^{1/2}$. If we assume that $\gamma\propto\hbar^{-1}$, as is the case for the harmonic oscillator,[47] then the magnitudes of the imaginary parts of these vectors scale as $\hbar^{1/2}$, and may be neglected as $\hbar\rightarrow0$. For the time-dependent difference phase variables in Eq. (31), $\Delta\mathbf{p}_{2n-2,2n-3}(t_{n-1})$ and $\Delta\mathbf{q}_{2n-2,2n-3}(t_{n-1})$, this $\hbar$ dependence scales a factor that diverges exponentially with t_{n-1} for a chaotic system and linearly for a regular system such as the one-dimensional Morse oscillator considered in Sec. III.[31] However, at any finite time value, these contributions can be neglected in the limit $\hbar\rightarrow0$, justifying the delta function approximation in Eq. (32). The prefactor of the delta function can be obtained by integrating Eq. (33) over $\overline{\mathbf{p}}_{ij}$ and $\overline{\mathbf{q}}_{ij}$ to obtain

$$\int\frac{d\overline{\mathbf{z}}_{ij}}{(2\pi\hbar)^F}\frac{\langle\mathbf{z}_a|\mathbf{z}_i\rangle\langle\mathbf{z}_j|\mathbf{z}_b\rangle}{\langle\mathbf{z}_j|\mathbf{z}_i\rangle}=\langle\mathbf{z}_a|\mathbf{z}_b\rangle. \tag{34}$$

Some ramifications of this result are discussed in Appendix B.

Application of the approximation in Eq. (32) to Eq. (31) permits the integration over the mean phase point, $\overline{\mathbf{z}}_{2n-1,2n}$, to be performed, and the integration over the difference phase point, $\Delta\mathbf{z}_{2n-1,2n}$, can then be carried out using the identity in Eq. (27) to give

$$J_{2n-3,2n-2}=\langle\mathbf{z}_{2n-2}(t_{n-1})|\mathbf{z}_{2n-3}(t_{n-1})\rangle$$
$$\times\frac{\partial q(\overline{\mathbf{z}}_{2n-3,2n-2}(t_{n-1}),t_n)}{\partial\overline{p}_{2n-3,2n-2}(t_{n-1})}. \tag{35}$$

In this relation, $q(\mathbf{z},t)$ represents the active coordinate at the end of a trajectory of duration t beginning at phase point $\mathbf{z}$. Repetition of this procedure $n-2$ times yields an expression with similar structure to the result for the linear response function in Eq. (24), and which reduces to Eq. (24) for $n=1$,

$$R^{(n)}(t_n,\ldots,t_1)=\int\frac{d\overline{\mathbf{z}}_{12}}{(2\pi\hbar)^F}\left(\frac{\partial^n q(\overline{\mathbf{z}}_{12},t_1+\cdots+t_n)}{\partial p(\overline{\mathbf{z}}_{12},t_1+\cdots+t_{n-1})\partial p(\overline{\mathbf{z}}_{12},t_1+\cdots+t_{n-2})\cdots\partial p(\overline{\mathbf{z}}_{12},0)}\right)$$
$$\times\int\frac{d\Delta\mathbf{z}_{12}}{(2\pi\hbar)^F}\frac{\langle\mathbf{z}_1|\hat{\rho}|\mathbf{z}_2\rangle}{\langle\mathbf{z}_1|\mathbf{z}_2\rangle}[G(\mathbf{z}_1,t_1)G^*(\mathbf{z}_2,t_1)\langle\mathbf{z}_2(t_1)|\mathbf{z}_1(t_1)\rangle\langle\mathbf{z}_1|\mathbf{z}_2\rangle]_{\rm lin}. \tag{36}$$

Here, $p(\mathbf{z},t)$ signifies the momentum of the active degree of freedom at the end of a trajectory of duration t, originating at phase point $\mathbf{z}$. The right-hand side of Eq. (36) vanishes at $n>1$ for a harmonic system, because of the vanishing of the nth momentum derivative of the coordinate in the integrand for this case. The correct classical mechanical limit of $R^{(n)}$ for any potential may then be extracted by following the argument applied to Eq. (24),

$$R^{(n)}(t_n,\ldots,t_1)=\int d\mathbf{z}\left(\frac{\partial^n q(\mathbf{z},t_1+\cdots+t_n)}{\partial p(\mathbf{z},t_1+\cdots+t_{n-1})\partial p(\mathbf{z},t_1+\cdots+t_{n-2})\cdots\partial p(\mathbf{z},0)}\right)f_{\rm cl}(\mathbf{z}). \tag{37}$$

The semiclassical nonlinear response function in Eq. (14) thus reduces to the correct classical limit for $\hbar \to 0$ and within the assumption that the coherent states spatial width parameter γ is taken to obey $\gamma \approx \hbar^{-1}$.

III. NUMERICAL RESULTS

A semiclassical expression for the nth order optical response function $R^{(n)}(t)$, based on the HK propagator, is given in Eq. (14). For a system of F degrees of freedom, its numerical evaluation requires calculation of a $4nF$-dimensional integral whose integrand requires the propagation of $2n$ classical trajectories. We provide a preliminary assessment of the accuracy of this approach with calculations of the linear response function $R^{(1)}(t)$ for a model of sufficient simplicity to allow classical mechanical, quantum mechanical, and semiclassical results to be readily computed and compared.

We consider a thermal ensemble of Morse oscillators,[57,58] with the Hamiltonian and density operator,

$$\hat{H} = \frac{\hat{p}^2}{2m} + D(1 - e^{-\alpha \hat{q}})^2, \tag{38}$$

$$\hat{\rho} = \frac{e^{-\beta \hat{H}}}{\mathrm{Tr}\, e^{-\beta \hat{H}}}. \tag{39}$$

Variables with dimensions of time will be scaled by the harmonic frequency of the oscillator, defined by

$$\omega = \alpha \sqrt{\frac{2D}{m}}. \tag{40}$$

The linear response function as defined in Eq. (2) has dimensions of the product of inverse mass and inverse angular frequency, and will be presented in units of $(m\omega)^{-1}$. For classical oscillators, the dimensionless $m\omega R^{(1)}(t)$, expressed as a function of ωt, is completely specified by one additional dimensionless parameter,[12–14] a temperature dependent anharmonicity, $\mathcal{F}$,

$$\mathcal{F} = \frac{6\alpha^3 D}{\beta^{1/2} m^{3/2} \omega^3} = \frac{3}{\sqrt{2\beta D}}. \tag{41}$$

The numerator of the expression after the first equality, $6\alpha^3 D$, is the cubic anharmonicity of the Morse potential. Specification of $m\omega R^{(1)}(t)$ for quantum oscillators requires an additional dimensionless parameter containing $\hbar$. For this parameter, we choose[15,16] the dimensionless quantum anharmonic frequency shift χ,

$$\chi = \frac{\mathcal{F}^2 \beta \hbar \omega}{9} = \frac{\hbar \omega}{2D}. \tag{42}$$

This quantity is the frequency difference between the $n \to n+1$ and $n+1 \to n+2$ transitions, scaled by ω. Another useful interpretation of χ is that the number of bound quantum states[58] for the Morse oscillator is the largest integer smaller than $\chi^{-1} - 1/2$. In the calculations below we will vary χ at fixed $\mathcal{F}$, which has the significance of varying the importance of $\hbar$ at fixed temperature, and we will vary $\mathcal{F}$ at fixed χ, with the significance of varying the temperature for fixed oscillator Hamiltonian.

The linear response function, within the approximation of the HK propagator, is given in Eq. (15). Numerical evaluation of this expression requires calculation of the matrix element between coherent states of the density operator. An exact calculation of this quantity, or one within an approximation consistent with the HK treatment of the dynamics,[59] is feasible for a single degree of freedom. However with a view towards future applications to larger systems, we will treat the density matrix in the simplest conceivable way by applying the high temperature limit of Eq. (28). With this additional approximation, the form of $R^{(1)}$ employed below for numerical calculations is

$$\begin{aligned} R_{\mathrm{sc}}^{(1)}(t) = \frac{\beta}{m} \int d\bar{z}_{12} f_{\mathrm{cl}}(\bar{z}_{12}) \bar{p}_{12}(0) \int \frac{d\Delta z_{12}}{2\pi\hbar} C(\bar{z}_{12} + \Delta z_{12}/2, t) C^*(\bar{z}_{12} - \Delta z_{12}/2, t) \\ \times \exp\left[\frac{i}{\hbar}\left(S(\bar{z}_{12} + \Delta z_{12}/2, t) - S(\bar{z}_{12} - \Delta z_{12}/2, t)\right)\right] \exp\left[\frac{i}{\hbar}\left(\bar{p}_{12}(0)\Delta q_{12}(0) - \bar{p}_{12}(t)\Delta q_{12}(t)\right)\right] \\ \times \exp\left[-\frac{\gamma}{4}\left(\Delta q_{12}^2(0) + \Delta q_{12}^2(t)\right) - \frac{1}{4\hbar^2\gamma}\left(\Delta p_{12}^2(0) + \Delta p_{12}^2(t)\right)\right]\left[\bar{q}_{12}(t) + \frac{i}{2\hbar\gamma}\Delta p_{12}(t)\right]. \end{aligned} \tag{43}$$

The classical phase space distribution is $f_{\mathrm{cl}}(z)$, the classical action (Hamilton's principal function) is $S(z,t)$, and the HK prefactor $C(z,t)$ is given in Eq. (5). For emphasis, mean and difference coordinates and momenta at $t=0$, $\bar{y}_{12}$ and Δy_{12}, are denoted $\bar{y}_{12}(0)$ and $\Delta y_{12}(0)$. A variety of sampling approaches may be envisioned for computing this four-dimensional integral by a Monte Carlo procedure.[60] We have chosen to sample the mean phase points $\bar{z}_{12}$ according to the classical phase space distribution and to sample the difference phase points Δz_{12} according to the Gaussian factor $\exp[-(\gamma/4)(\Delta q_{12}^2(0)) - (1/4\hbar^2\gamma)(\Delta p_{12}^2(0))]$. Since our interest lies with the response of a bound, anharmonic system, we choose temperatures such that initial phase points with energies exceeding the well depth D are improbable, and we

discard the negligible fraction of initial conditions with energy larger than D. The trajectories $z_1(t)$ and $z_2(t)$ are propagated numerically with the velocity Verlet algorithm.[61] The action $S(z_j,t)$ and monodromy matrix are propagated by applying the velocity Verlet algorithm to the equations of motion,

$$\dot{S}(z_j,t)=L(q_j,\dot{q}_j,t), \tag{44}$$

$$\begin{bmatrix} \dot{M}_{qq}(t) & \dot{M}_{qp}(t) \\ \dot{M}_{pq}(t) & \dot{M}_{pp}(t) \end{bmatrix} = \begin{bmatrix} 0 & -m^{-1} \\ V_{qq}(t) & 0 \end{bmatrix} \begin{bmatrix} M_{qq}(t) & M_{qp}(t) \\ M_{pq}(t) & M_{pp}(t) \end{bmatrix}. \tag{45}$$

In Eq. (44), the Lagrangian is denoted L. The curvature of the potential energy is represented by V_{qq} in Eq. (45). The HK prefactor $C(z,t)$ in Eq. (5) is computed from the monodromy matrix. While the use of the HK propagator obviates the need to calculate the Morse–Maslov index required by the Van Vleck propagator, the square root in Eq. (5) must be computed with a continuous phase. The continuity of this phase is ensured by incrementing the phase of $C(z,t)$ by π each time the determinant in Eq. (5) crosses over the principal branch of the square root function.

Use of the HK propagator requires specifying the value of γ, the spatial width parameter characterizing the coherent states, which in principle can be taken to have any value. In keeping with the spirit of derivations of the HK propagator,[21,45,46,62] we assign to this parameter a value very close to its exact value for a harmonic oscillator, $\gamma_{\mathrm{HO}} \equiv m\omega/\hbar$. In the calculations shown below in Figs. 3–6, $\gamma = 0.978\gamma_{\mathrm{HO}}$. The effect of varying the value of γ on the calculation of $R^{(1)}$ is discussed below in connection with Fig. 7.

Semiclassical calculations of $R^{(1)}$ are compared below to classical and quantum results. The classical $R^{(1)}$ is computed from Eq. (29), rewritten as

$$R_c^{(1)}(t)=\frac{\beta}{m}\int dz f_{\mathrm{cl}}(z)q(t)p(0). \tag{46}$$

Initial conditions for classical trajectories are sampled according to $f_{\mathrm{cl}}(z)$, with dissociative trajectories discarded as described above in connection with $R_{\mathrm{sc}}^{(1)}$. Rather than propagating the trajectories numerically as in the calculation of $R_{\mathrm{sc}}^{(1)}$, we have taken advantage of the analytical solution of Morse oscillator dynamics in terms of action-angle variables.[57,58] The action I and angle ϕ are defined in terms of q and p by

$$I(q,p)=\frac{2D}{\omega}(1-\lambda), \tag{47}$$

$$\phi(q,p)=-\arctan\frac{p\lambda}{\sqrt{2mD}(\lambda^2-e^{-\alpha q})}, \tag{48}$$

$$\lambda=\sqrt{1-H(q,p)/D}. \tag{49}$$

The classical Hamiltonian is denoted $H(q,p)$. We evaluate $R_c^{(1)}$ by generating initial values of q and p, calculating the corresponding action $I(p,q)$ and initial angle $\phi(q,p)$, propagating the angle according to $\phi\rightarrow\phi+\lambda\omega t$, and computing $q(t)$ and $p(t)$ from

$$q(I,\phi)=\alpha^{-1}\ln[\lambda^{-2}(1+b\cos\phi)], \tag{50}$$

$$p(I,\phi)=-\frac{m\omega\lambda b}{\alpha}\frac{\sin\phi}{1+b\cos\phi}, \tag{51}$$

$$b=\sqrt{H(p,q)/D}. \tag{52}$$

These relations follow from Eqs. (4) and (8) in the paper by Shirts,[58] with the replacement $\Theta\rightarrow-\phi$.

The quantum response function is computed from Eq. (2) with $n=1$,

$$R_q^{(1)}(t)=\frac{i}{\hbar}\mathrm{Tr}\{\hat{x}(t)[\hat{x},\hat{\rho}]\}. \tag{53}$$

The trace is evaluated in the energy representation, with coordinate matrix elements computed as described, for example, in Eq. (33) of the paper by Shirts.[58] We approximate the resulting sums over eigenstates to include only bound states, just as we discarded dissociative trajectories in calculating the classical and semiclassical response functions.

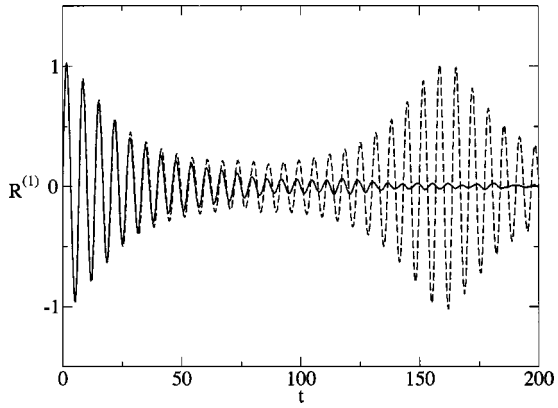

FIG. 3. Classical (solid curve) and quantum (dashed curve) linear response functions for a thermal distribution of Morse oscillators are shown for anharmonicity $\mathcal{F}=0.594$. The quantum case has anharmonic frequency shift $\chi=0.0391$.

The solid curve in Fig. 3 shows the classical mechanical $R^{(1)}(t)$, computed from Eq. (46) for $\mathcal{F}=0.594$. This value represents a substantial anharmonicity. For example, the vibration of CO, a chromophore in vibrational echo measurements,[2–4] has $\mathcal{F}\approx 0.1$ at room temperature. The response function is characterized by an oscillation at a frequency close to ω and a decay associated with interference from contributions of different energies in the thermal distribution of initial conditions. The dashed curve in Fig. 3 shows a quantum calculation from Eq. (53) for the same value of $\mathcal{F}$ and $\chi=0.0391$. This value of χ corresponds to a Morse oscillator with 25 bound states, $\beta\hbar\omega=1$, and $\beta D=12.775$. Quantum and classical results agree well for the first few oscillations and differ primarily in two respects. The quantum response function shows a recurrence with approximate period $2\pi/\chi$, reflecting the constant anharmonic frequency shift between successive one quantum transitions in the Morse oscillator. In addition, there is a frequency shift be-

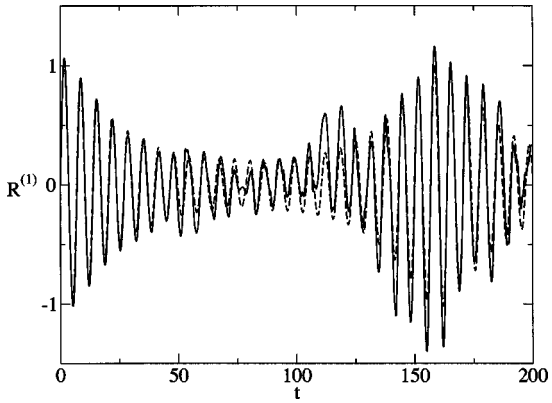

FIG. 4. Quantum (dashed curve) and semiclassical (solid curve) linear response functions for a thermal distribution of Morse oscillators are shown for the conditions of Fig. 3, $\mathcal{F}=0.594$ and $\chi=0.0391$.

tween the rapid oscillations in the quantum and classical responses, with the classical response displaying a higher frequency.

Wu and Cao have compared quantum and classical nonlinear response functions for the Morse oscillator with a different model of radiation–matter coupling and different choice of initial conditions from those treated here.[55] The radiation–matter coupling is taken to be quadratic in electric field, so that the third-order and fifth-order response functions treated in that work have, respectively, an analogous structure to the linear and second-order response functions in our formalism. Also, the radiation-matter coupling is taken to be linear in creation and annihilation operators for the Morse oscillator, which does not correspond to any single power of the oscillator coordinate. Wu and Cao compared quantum and classical third-order response functions for a microcanonical initial condition. The classical calculation is characterized by a linear divergence,[63] associated with the linear growth of stability derivatives, while the quantum calculation shows a slow oscillation at the anharmonic frequency shift. Wu and Cao also computed classical response functions using an initial condition of a uniform distribution in classical action, of width $\hbar$. Averaging over a distribution with this particular discontinuous form is shown to destroy the linear divergence, and produce an oscillatory result closely resembling the quantum response function. In fact, the form of the polarization operator used by Wu and Cao, which effectively obeys harmonic oscillator selection rules in an anharmonic system, together with the discontinuous phase space distribution function, ensures that the classical and quantum response functions are essentially identical. The calculations in our Fig. 3 are representative of the significant differences between the classical and quantum responses, in particular, the lack of classical recurrence at longer times, to be expected for thermal or other smooth distributions of anharmonic oscillators.

The dashed curve in Fig. 4 reproduces from Fig. 3 the quantum response function for $\mathcal{F}=0.594$ and $\chi=0.0391$, and the solid curve shows the semiclassical result computed from Eq. (43). The semiclassical calculation, based on the HK propagator and a high temperature approximation for the density matrix, reproduces the two primary features of the

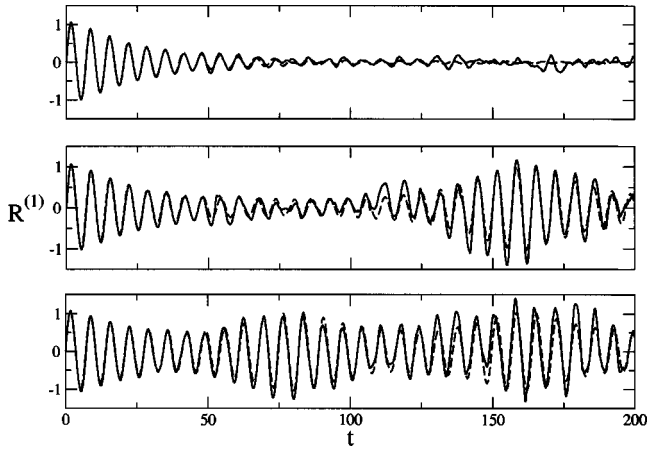

FIG. 5. The dependence of the linear response function on the number of bound states in the Morse oscillator is shown for quantum (dashed curves) and semiclassical (solid curves) calculations. $\mathcal{F}=0.594$. In the upper panel, $\chi=0.00391$ (255 bound states), in the middle panel, $\chi=0.0391$ (25 bound states), and in the lower panel, $\chi=0.0782$ (12 bound states).

quantum result: the recurrence at $2\pi/\chi$ and the frequency shift of the rapid oscillations with respect to the classical result.

The dependence of the linear response function on the importance of $\hbar$ is shown by the solid (semiclassical) and dashed (quantum) curves in the three panels of Fig. 5 for $\chi=0.00391$ (upper panel), $\chi=0.0391$ (middle panel), and $\chi=0.0782$ (lowest panel). The numbers of bound quantum states in each case are, respectively, 255 (upper panel), 25 (middle panel), and 12 (lowest panel). The period of the recurrence in the quantum result is shown to be inversely proportional to χ, as discussed above, and the semiclassical calculation is shown to be qualitatively correct for Morse oscillators with varying number of bound states.

The temperature dependence of $R^{(1)}(t)$ is displayed in Fig. 6. The upper panel reproduces from the middle panel of Fig. 4 quantum (dashed) and semiclassical (solid) response functions for $\mathcal{F}=0.594$ and $\chi=0.0391$. In the middle panel

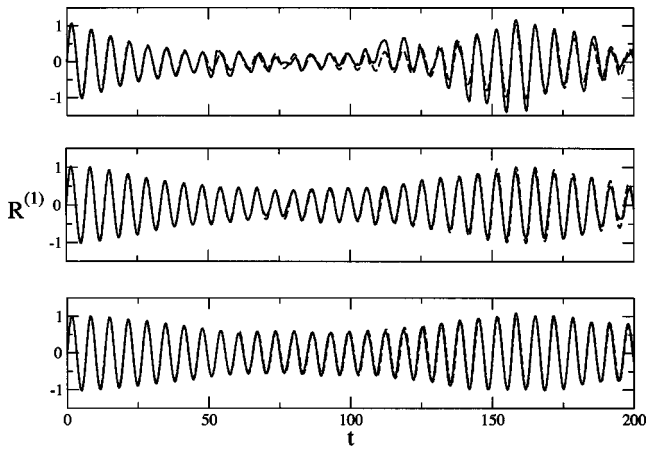

FIG. 6. The dependence of the linear response function on temperature is shown for quantum (dashed curves) and semiclassical (solid curves) calculations. In the upper panel, $\mathcal{F}=0.594$ and $\chi=0.0391$, in the middle panel the temperature has been reduced to $\mathcal{F}=0.485$, and in the lowest panel, temperature has been further reduced to $\mathcal{F}=0.420$.

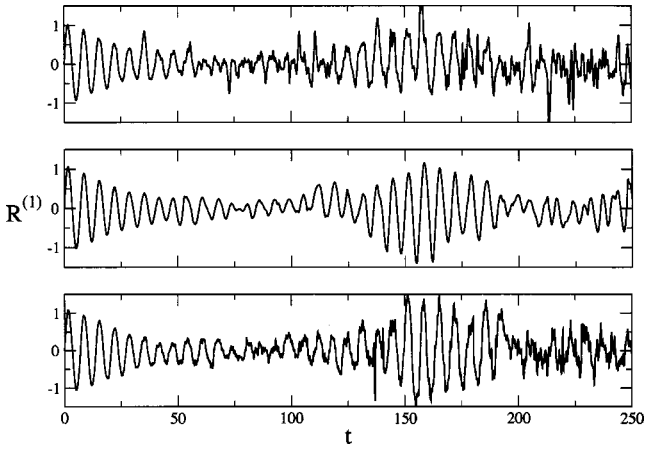

FIG. 7. The dependence of the semiclassical linear response function on the coherent states spatial width parameter, γ, is shown for $\mathcal{F}=0.594$ and $\chi=0.0391$. In the middle panel, $\gamma=0.978\gamma_{\mathrm{HO}}$, and is increased to $\gamma=3.91\gamma_{\mathrm{HO}}$ in the upper panel and decreased to $\gamma=0.245\gamma_{\mathrm{HO}}$ in the lower panel.

with $\mathcal{F}=0.485$, the temperature is reduced to 2/3 of the value in the upper panel, and in the lowest panel with $\mathcal{F}=0.420$, the temperature is further reduced to half of the value in the upper panel. As discussed above, the period of the recurrence in the quantum calculations is unaffected by temperature, but the initial decay rate of the envelope of $R^{(1)}$ increases with increasing temperature. These trends are reproduced by the semiclassical calculations. The calculations shown in the lowest panels of Figs. 5 and 6 represent the rather low temperature, $\beta\hbar\omega=2$, with $\beta D=12.75$ in the lowest panel of Fig. 5 and $\beta D=25.5$ in the lowest panel of Fig. 6. It is remarkable that the semiclassical expression in Eq. (43) remains accurate at these low temperatures, as it includes the nominally high-temperature approximation to the density matrix of Eq. (28).

The dependence of the semiclassical $R^{(1)}$ on the coherent states spatial width parameter γ is shown in Fig. 7 for $\mathcal{F}=0.594$ and $\chi=0.0391$. The middle panel shows $R^{(1)}$ for $\gamma=0.978\gamma_{\mathrm{HO}}$, the value employed in Figs. 3–6. In the upper panel, γ is increased to $\gamma=3.91\gamma_{\mathrm{HO}}$, and in the lower panel it is decreased to $\gamma=0.245\gamma_{\mathrm{HO}}$. Each curve was calculated from 25 000 trajectories of duration $250\omega^{-1}$ and integration time step $0.01\omega^{-1}$, which are comparable statistics to those of the calculations shown in Figs. 4–6. The accuracy and efficiency of convergence of the semiclassical calculation are shown to degrade for values of γ that differ substantially from the harmonic oscillator value.[39] It should be recalled from Sec. II that $R^{(1)}_{\mathrm{sc}}(t)$ for a harmonic oscillator is independent of the value of γ, suggesting that the sensitivity of the calculation to choice of γ depends on degree of anharmonicity.

IV. CONCLUSIONS

We have treated a rather general model of the radiation-matter interaction, in which a classical electric field is coupled to matter with an interaction that is linear in the coordinate of an ''active'' degree of freedom, which in turn interacts with $F-1$ other material degrees of freedom. We have developed a compact expression for the nth order material response function, based on the Herman–Kluk semiclassical approximation to the quantum propagator. This form for $R^{(n)}$ lends itself to the extraction of the correct classical mechanical limit, thereby providing insight into the relationship between classical and quantum response functions.

As a preliminary test of the accuracy of the application of the HK propagator to the calculation of optical response functions, we have computed the linear response of a thermal distribution of Morse oscillators. These calculations, shown in Figs. 4–7, employ a high temperature approximation to the density matrix, in addition to the HK approximation to the propagator. The semiclassical calculations of $R^{(1)}$ presented here reproduce the important characteristics that distinguish quantum from classical calculations of this observable.

Of course, the motivation for developing a semiclassical treatment of nonlinear optical response is the application to systems with F too large to treat with quantum mechanics. The semiclassical calculation of $R^{(n)}$ with coherent states requires evaluation of a $4nF$-dimensional integral with an integrand that involves calculating $2n$ classical trajectories and associated stability matrices. For example, extending the calculations of the linear response of the Morse oscillator model treated here to compute the vibrational echo,[12–16] requires $R^{(3)}$ and hence the evaluation of a 12-dimensional integral. Calculating semiclassical higher order response functions for systems with more degrees of freedom will require a considered choice of the Monte Carlo sampling algorithm employed.[60] The well-known difficulty of computing high dimensional integrals of oscillatory integrands with Monte Carlo approaches[60] suggests that further approximations, in addition to the two employed here, will be required to simplify the structure of $R^{(n)}$ that is depicted in the diagram in Fig. 1. While we leave such considerations for future work, the calculations shown here suggest promise for the semiclassical treatment of $R^{(n)}$ based on the HK propagator.

ACKNOWLEDGMENTS

The authors thank Professor M. F. Herman for a helpful discussion concerning the identity of Eq. (27). W.G.N. thanks the National Science Foundation for support through a Graduate Research Fellowship. R.F.L. acknowledges support from the National Science Foundation through Grant No. CHE0105623, and from the Petroleum Research Fund of the American Chemical Society.

APPENDIX A: RESPONSE FUNCTIONS IN COORDINATE REPRESENTATION

In this Appendix we derive semiclassical expressions for linear and nonlinear response functions using the coordinate representation, employing the Van Vleck[17,18,23] rather than the Herman–Kluk[21,22] semiclassical propagator. The classical limit of our semiclassical result is obtained by a linearization approximation.[29,48,50,53,64] While the classical limit of operator correlation functions has previously been discussed using the Van Vleck propagator together with linearization of the semiclassical expression,[48] the results obtained here pro-

vide an explicit demonstration of the emergence of multitime classical Poisson brackets[11] from the quantum mechanical nested commutator structure. For related treatments of the nonlinear response function, see the work of Mukamel *et al.*[11,65–67] An analogous proof of the emergence of the classical limit using the HK propagator is given in Sec. II.

As in Sec. II, we take the system to have F coordinate degrees of freedom, $\{(\mathbf{r})_i, i=0,\ldots,F-1\}$, with the single active degree of freedom denoted $x\equiv(\mathbf{r})_0$. The Van Vleck semiclassical approximation to the quantum mechanical propagator $K(\mathbf{r}',\mathbf{r};t)\equiv\langle\mathbf{r}'|\hat{K}(t)|\mathbf{r}\rangle$ is[17,18,23]

$$K_{VV}(\mathbf{r}',\mathbf{r};t)=\sqrt{\frac{1}{(2\pi i\hbar)^F}}\sum_k \sqrt{C_{VV}(\mathbf{r}',\mathbf{r};t)} \times\exp\left[\frac{iS(\mathbf{r}',\mathbf{r};t)}{\hbar}-i\mu\frac{\pi}{2}\right], \tag{A1}$$

where the sum includes all distinct classical trajectories k connecting $\mathbf{r}$ to $\mathbf{r}'$ in time t, $S(\mathbf{r}',\mathbf{r};t)$ is the associated classical action (Hamilton's principal function),[23] the prefactor

$$C_{VV}(\mathbf{r}',\mathbf{r};t)\equiv\left|\det\left[\frac{\partial\mathbf{p}}{\partial\mathbf{r}'}\right]\right|=\left|\det\left[-\frac{\partial^2 S}{\partial\mathbf{r}\partial\mathbf{r}'}\right]\right|, \tag{A2}$$

and μ is the Morse–Maslov index.[23]

1. Linear response function

The linear response function $R^{(1)}$ is given in Eq. (2) with $n=1$,

$$R^{(1)}(t)=\left(\frac{i}{\hbar}\right)\mathrm{Tr}\{\hat{x}(t)[\hat{x},\hat{\rho}]\} =\left(\frac{i}{\hbar}\right)\mathrm{Tr}\{\hat{K}(t)^\dagger\hat{x}\hat{K}(t)\hat{x}\hat{\rho}-\hat{x}\hat{K}(t)^\dagger\hat{x}\hat{K}(t)\hat{\rho}\}. \tag{A3}$$

Inserting complete sets of position eigenstates $|\mathbf{r}\rangle$, and using $\hat{x}|\mathbf{r}\rangle=x|\mathbf{r}\rangle$, we have

$$R^{(1)}(t)=\left(\frac{i}{\hbar}\right)\int d\mathbf{r}_1\int d\mathbf{r}_0''\int d\mathbf{r}_0' K(\mathbf{r}_1,\mathbf{r}_0';t)^* \times K(\mathbf{r}_1,\mathbf{r}_0'';t)x_1(x_0''-x_0')\langle\mathbf{r}_0''|\hat{\rho}|\mathbf{r}_0'\rangle. \tag{A4}$$

We now introduce the transformation to average and difference coordinates

$$\overline{\mathbf{R}}_0\equiv\frac{(\mathbf{r}_0''+\mathbf{r}_0')}{2},\quad \Delta\mathbf{R}_0\equiv\mathbf{r}_0''-\mathbf{r}_0', \tag{A5}$$

and express the coordinate-space representation matrix elements of the density operator in terms of the Wigner distribution,[68] $\rho_W(\mathbf{q},\mathbf{p})$,

$$\langle\mathbf{r}_0''|\hat{\rho}|\mathbf{r}_0'\rangle=\int d\mathbf{P}_0 e^{(i/\hbar)\,\mathbf{P}_0\cdot\Delta\mathbf{R}_0}\rho_W(\overline{\mathbf{R}}_0,\mathbf{P}_0). \tag{A6}$$

Equation (A1) is then used, omitting the sum over distinct trajectories k for simplicity, and suppressing the Morse–Maslov phases, which cancel in the classical limit, to obtain a semiclassical approximation for $R^{(1)}(t)$,

$$R^{(1)}(t)=\left(\frac{i}{\hbar}\right)\frac{1}{(2\pi\hbar)^F}\int d\mathbf{r}_1\int d\overline{\mathbf{R}}_0\int d\Delta\mathbf{R}_0\int d\mathbf{P}_0 \times\sqrt{\left|\det\left[\frac{\partial\mathbf{p}_0''}{\partial\mathbf{r}_1}\right]\right|}\sqrt{\left|\det\left[\frac{\partial\mathbf{p}_0'}{\partial\mathbf{r}_1}\right]\right|} \times x_1\Delta X_0\rho_W(\overline{\mathbf{R}}_0,\mathbf{P}_0) \times e^{i[S(\mathbf{r}_1,\mathbf{r}_0'';t)-S(\mathbf{r}_1,\mathbf{r}_0';t)]/\hbar}e^{i\mathbf{P}_0\cdot\Delta\mathbf{R}_0/\hbar}. \tag{A7}$$

The semiclassical expression (A7) for the linear response function can in principle be evaluated via numerical computation of the multiple integrals involved. Finding pairs of classical trajectories of duration t connecting initial configurations $\mathbf{r}_0'$ and $\mathbf{r}_0''$ to the same final configuration $\mathbf{r}_1$ constitutes a difficult root search problem. An initial value representation (IVR) expression[29] for $R^{(1)}$ can be obtained by replacing the integration over variables $\{\mathbf{r}_0',\mathbf{r}_0'',\mathbf{r}_1\}$ with an integration over initial coordinate-momentum pairs $\{\mathbf{r}_0'',\mathbf{p}_0''\}$ for forward trajectories from $\mathbf{r}_0''$ to $\mathbf{r}_1(\mathbf{r}_0'',\mathbf{p}_0'';t)$, together with an integration over momenta $\mathbf{p}_1$, where $\mathbf{r}_1,\mathbf{p}_1$ serve as the initial conditions for trajectories propagated backwards in time to $\mathbf{r}_0'$ at $t=0$. The Van Vleck propagator exhibits divergences associated with trajectory conjugate points;[23] use of the semiclassical IVR overcomes the difficulties associated with this singular behavior.[27,29]

In order to extract the classical response function from the semiclassical result (A7), we introduce the key linearization approximation.[29] Expanding the action difference appearing in the exponent in Eq. (A7) to second order in $\Delta\mathbf{R}$ we obtain

$$S(\mathbf{r}_1,\mathbf{r}_0'';t)-S(\mathbf{r}_1,\mathbf{r}_0';t)\simeq-\overline{\mathbf{p}}_0\cdot\Delta\mathbf{R}_0+\cdots, \tag{A8}$$

with

$$\overline{\mathbf{p}}_0\equiv-\left.\frac{\partial S(\mathbf{r}_1,\overline{\mathbf{R}}_0;t)}{\partial\overline{\mathbf{R}}_0}\right|_{\mathbf{r}_1}, \tag{A9}$$

the initial momentum for the classical trajectory connecting the mean initial position $\overline{\mathbf{R}}_0$ to $\mathbf{r}_1$ in time t. Also, we replace each prefactor with that for the mean trajectory,

$$\left|\det\left[\frac{\partial\mathbf{p}_0'}{\partial\mathbf{r}_1}\right]\right|\simeq\left|\det\left[\frac{\partial\mathbf{p}_0''}{\partial\mathbf{r}_1}\right]\right|\simeq\left|\det\left[\frac{\partial\overline{\mathbf{p}}_0}{\partial\mathbf{r}_1}\right]\right|, \tag{A10}$$

so that the semiclassical expression (A7) becomes

$$R^{(1)}(t)=\left(\frac{i}{\hbar}\right)\frac{1}{(2\pi\hbar)^F}\int d\mathbf{r}_1\int d\overline{\mathbf{R}}_0\int d\Delta\mathbf{R}_0\int d\mathbf{P}_0 \times\left|\det\left[\frac{\partial\overline{\mathbf{p}}_0}{\partial\mathbf{r}_1}\right]\right|x_1\Delta X_0 e^{i(\mathbf{P}_0-\overline{\mathbf{p}}_0)\cdot\Delta\mathbf{R}_0/\hbar}\rho_W(\overline{\mathbf{R}}_0,\mathbf{P}_0). \tag{A11}$$

This result expresses the linear response function as an integral over all coordinate pairs $(\overline{\mathbf{R}}_0,\ \mathbf{r}_1)$ connected by classical trajectories of duration t and initial momentum $\overline{\mathbf{p}}_0$, together with integrations over difference coordinate $\Delta\mathbf{R}_0$ and momentum variable $\mathbf{P}_0$.

We can integrate over $\Delta\mathbf{R}_0$ and apply the integral representation of the delta function to obtain

$$R^{(1)}(t)=-\int d\mathbf{r}_1\int d\overline{\mathbf{R}}_0\int d\mathbf{P}_0\left|\det\left[\frac{\partial\overline{\mathbf{p}}_0}{\partial\mathbf{r}_1}\right]\right| \times x_1\left[\frac{\partial\delta(P_0-\overline{p}_0)}{\partial\overline{p}_0}\right] \times\prod_{\alpha=1}^{F-1}\delta((\mathbf{P}_0)_\alpha-(\overline{\mathbf{p}}_0)_\alpha)\rho_W(\overline{\mathbf{R}}_0,\mathbf{P}_0), \tag{A12}$$

where $\overline{P}_0\equiv(\overline{\mathbf{P}}_0)_0$, etc. The final coordinate $\mathbf{r}_1$ is a function of $\overline{\mathbf{R}}_0$ and $\overline{\mathbf{p}}_0$, $\mathbf{r}_1=\mathbf{r}_1(\overline{\mathbf{R}}_0,\overline{\mathbf{p}}_0)$, so that we have

$$\int d\mathbf{r}_1\left|\det\left[\frac{\partial\overline{\mathbf{p}}_0}{\partial\mathbf{r}_1}\right]\right|f(\mathbf{r}_1)\left[\frac{\partial\delta(P_0-\overline{p}_0)}{\partial\overline{p}_0}\right]\prod_{\alpha=1}^{F-1}\delta((\mathbf{P}_0)_\alpha-(\overline{\mathbf{p}}_0)_\alpha) =-\left.\frac{\partial f(\mathbf{r}_1(\overline{\mathbf{R}}_0,\overline{\mathbf{p}}_0))}{\partial\overline{p}_0}\right|_{\overline{\mathbf{p}}_0=\mathbf{P}_0} \tag{A13}$$

and

$$R^{(1)}(t)=\int d\overline{\mathbf{R}}_0\int d\mathbf{P}_0\frac{\partial x_1(\overline{\mathbf{R}}_0,\mathbf{P}_0;t)}{\partial P_0}\rho_W(\overline{\mathbf{R}}_0,\mathbf{P}_0). \tag{A14}$$

Recognizing the partial derivative in the integrand as a 2-time classical Poisson bracket,

$$\frac{\partial x_1(\mathbf{R}_0,\mathbf{P}_0;t)}{\partial P_0}=-\{x(t),x(0)\}|_{\mathbf{r}(0)=\mathbf{R}_0,\mathbf{p}(0)=\mathbf{P}_0}, \tag{A15}$$

we obtain finally

$$R^{(1)}(t)=\int d\mathbf{R}_0\int d\mathbf{P}_0\{x(0),x(t)\}\rho_W(\mathbf{R}_0,\mathbf{P}_0). \tag{A16}$$

This result expresses the linear response function $R^{(1)}(t)$ as the phase space average of the 2-time Poisson bracket $\{x(0),x(t)\}$ weighted by the equilibrium Wigner distribution function (cf. the LSC Wigner model[29]). Replacing the Wigner function ρ_W in Eq. (A16) with the classical phase space distribution function $f_{\rm cl}$ in the $\hbar\to0$ limit yields the classical result.

2. Nonlinear response function: Second order

To illustrate the derivation of a semiclassical expression for the nonlinear response function and the corresponding classical limit, we consider the first nonlinear response function, $R^{(2)}$ [cf. Eq. (2)],

$$R^{(2)}(t_2,t_1)\equiv\left(\frac{i}{\hbar}\right)^2\mathrm{Tr}\{\hat{x}(t_2+t_1)[\hat{x}(t_1),[\hat{x},\hat{\rho}]]\} =\left(\frac{i}{\hbar}\right)^2\mathrm{Tr}\{[[\hat{x}(t_2+t_1),\hat{x}(t_1)],\hat{x}]\hat{\rho}\}. \tag{A17}$$

Expanding the two nested commutators yields 4 terms,

$$\begin{aligned}R^{(2)}(t_2,t_1)=\left(\frac{i}{\hbar}\right)^2\mathrm{Tr}\{&\hat{K}(t_2+t_1)^\dagger\hat{x}\hat{K}(t_2)\hat{x}\hat{K}(t_1)\hat{x}\hat{\rho}-\hat{K}(t_2\\&+t_1)^\dagger\hat{x}\hat{K}(t_2)\hat{x}\hat{K}(t_1)\hat{\rho}\hat{x}\\&+\hat{K}(t_2+t_1)^\dagger\hat{x}\hat{K}(t_2+t_1)\hat{\rho}\hat{x}\hat{K}(t_1)^\dagger\hat{x}\hat{K}(t_1)\\&-\hat{K}(t_2+t_1)^\dagger\hat{x}\hat{K}(t_2+t_1)\hat{x}\hat{\rho}\hat{K}(t_1)^\dagger\hat{x}\hat{K}(t_1)\}.\end{aligned} \tag{A18}$$

Inserting complete sets of position eigenstates as before, we have

$$\begin{aligned}R^{(2)}(t_2,t_1)=\left(\frac{i}{\hbar}\right)^2\int d\mathbf{r}_2\int d\mathbf{r}_1'\int d\mathbf{r}_1''\int d\mathbf{r}_0'\int d\mathbf{r}_0''\\\times\langle\mathbf{r}_0''|\hat{\rho}|\mathbf{r}_0'\rangle K(\mathbf{r}_2,\mathbf{r}_1';t_2)^*K(\mathbf{r}_2,\mathbf{r}_1'';t_2)\\\times K(\mathbf{r}_1',\mathbf{r}_0';t_1)^*K(\mathbf{r}_1'',\mathbf{r}_0'';t_1)x_2(x_1''-x_1')\\\times(x_0''-x_0'),\end{aligned} \tag{A19}$$

where the product of difference coordinates in Eq. (A19) precisely mirrors the nested commutator structure in Eq. (A17). With the transformation to the average/difference coordinates in Eq. (A5) to introduce the Wigner function ρ_W, Eq. (A19) becomes

$$\begin{aligned}R^{(2)}(t_2,t_1)=\left(\frac{i}{\hbar}\right)^2\int d\mathbf{r}_2\int d\mathbf{r}_1'\int d\mathbf{r}_1''\int d\overline{\mathbf{R}}_0\int d\Delta\mathbf{R}_0\\\times\int d\mathbf{P}_0e^{i\mathbf{P}_0\cdot\Delta\mathbf{R}_0/\hbar}\rho_W(\overline{\mathbf{R}}_0,\mathbf{P}_0)\\\times K(\mathbf{r}_2,\mathbf{r}_1';t_2)^*K(\mathbf{r}_2,\mathbf{r}_1'';t_2)K(\mathbf{r}_1',\mathbf{r}_0';t_1)^*\\\times K(\mathbf{r}_1'',\mathbf{r}_0'';t_1)x_2(x_1''-x_1')(x_0''-x_0').\end{aligned} \tag{A20}$$

Replacing the quantum propagators K in Eq. (A20) with the Van Vleck propagator, K_{VV}, and introducing average/difference coordinates at the intermediate time $t=t_1$,

$$\overline{\mathbf{R}}_1\equiv\frac{(\mathbf{r}_1''+\mathbf{r}_1')}{2},\quad\Delta\mathbf{R}_1\equiv\mathbf{r}_1''-\mathbf{r}_1' \tag{A21}$$

we obtain

$$\begin{aligned}R^{(2)}(t_2,t_1)=\left(\frac{i}{\hbar}\right)^2\frac{1}{(2\pi\hbar)^{2F}}\int d\mathbf{r}_2\int d\overline{\mathbf{R}}_1\int d\Delta\mathbf{R}_1\int d\overline{\mathbf{R}}_0\int d\Delta\mathbf{R}_0\int d\mathbf{P}_0e^{i\mathbf{P}_0\cdot\Delta\mathbf{R}_0/\hbar}\\\times\sqrt{\left|\det\left[\frac{\partial\mathbf{p}_1''}{\partial\mathbf{r}_2}\right]\right|}\sqrt{\left|\det\left[\frac{\partial\mathbf{p}_1'}{\partial\mathbf{r}_2}\right]\right|}e^{i[S(\mathbf{r}_2,\mathbf{r}_1'';t_2)-S(\mathbf{r}_2,\mathbf{r}_1';t_2)]/\hbar}\sqrt{\left|\det\left[\frac{\partial\mathbf{p}_0''}{\partial\mathbf{r}_1''}\right]\right|}\sqrt{\left|\det\left[\frac{\partial\mathbf{p}_0'}{\partial\mathbf{r}_1'}\right]\right|}\\\times e^{i[S(\mathbf{r}_1'',\mathbf{r}_0'';t_1)-S(\mathbf{r}_1',\mathbf{r}_0';t_1)]/\hbar}\rho_W(\overline{\mathbf{R}}_0,\mathbf{P}_0)x_2\Delta X_1\Delta X_0,\end{aligned} \tag{A22}$$

where

$$\mathbf{p}_0''=-\left(\frac{\partial S(\mathbf{r}_1'',\mathbf{r}_0'';t_1)}{\partial \mathbf{r}_0''}\right)_{\mathbf{r}_1''}, \tag{A23}$$

and so on.

Again, this semiclassical expression could in principle be evaluated by numerical evaluation of the relevant multidimensional integral. The root search problem involves determination of classical trajectories connecting $\mathbf{r}_0'\rightarrow\mathbf{r}_1'$ and $\mathbf{r}_0''\rightarrow\mathbf{r}_1''$ in time t_1, and $\mathbf{r}_1'\rightarrow\mathbf{r}_2$ and $\mathbf{r}_1''\rightarrow\mathbf{r}_2$ in time t_2. Changing variables from initial and final coordinate pairs to inital coordinate-momentum pairs for each trajectory segment yields a semiclassical IVR Van Vleck expression for $R^{(2)}$,

$$\begin{aligned}R^{(2)}(t_2,t_1)=&\left(\frac{i}{\hbar}\right)^2\frac{1}{(2\pi\hbar)^{2F}}\int d\mathbf{p}_1'\int d\mathbf{p}_1''\int d\mathbf{r}_0'\int d\mathbf{p}_0'\int d\mathbf{r}_0''\int d\mathbf{p}_0''\,\delta(\mathbf{r}_2'-\mathbf{r}_2'')\\&\times\sqrt{\left|\det\left[\frac{\partial\mathbf{r}_2''}{\partial\mathbf{p}_1''}\right]\right|}\sqrt{\left|\det\left[\frac{\partial\mathbf{r}_2'}{\partial\mathbf{p}_1'}\right]\right|}\sqrt{\left|\det\left[\frac{\partial\mathbf{r}_1''}{\partial\mathbf{p}_0''}\right]\right|}\sqrt{\left|\det\left[\frac{\partial\mathbf{r}_1'}{\partial\mathbf{p}_0'}\right]\right|}\\&\times e^{i[S(\mathbf{p}_1'',\mathbf{r}_1'';t_2)-S(\mathbf{p}_1',\mathbf{r}_1';t_2)]/\hbar}e^{i[S(\mathbf{p}_0'',\mathbf{r}_0'';t_1)-S(\mathbf{p}_0',\mathbf{r}_0';t_1)]/\hbar}\langle\mathbf{r}_0''|\hat{\rho}|\mathbf{r}_0'\rangle x_2'(x_1''-x_1')(x_0''-x_0').\end{aligned} \tag{A24}$$

In order to retrieve the classical nonlinear response function from the semiclassical result (A22), we again linearize the actions, so that

$$S(\mathbf{r}_1'',\mathbf{r}_0'';t_1)-S(\mathbf{r}_1',\mathbf{r}_0';t_1)\simeq\overline{\mathbf{p}}_1(10)\cdot\Delta\mathbf{R}_1-\overline{\mathbf{p}}_0\cdot\Delta\mathbf{R}_0+\cdots, \tag{A25}$$

where $\overline{\mathbf{p}}_0$ is defined as above, and

$$\overline{\mathbf{p}}_1(10)\equiv\left(\frac{\partial S(\overline{\mathbf{R}}_1,\overline{\mathbf{R}}_0;t_1)}{\partial\overline{\mathbf{R}}_1}\right)_{\overline{\mathbf{R}}_0}, \tag{A26}$$

the final momentum for a classical trajectory connecting $\overline{\mathbf{R}}_0$ and $\overline{\mathbf{R}}_1$ in time t_1. Similarly,

$$S(\mathbf{r}_2,\mathbf{r}_1'';t_2)-S(\mathbf{r}_2,\mathbf{r}_1';t_2)\simeq-\overline{\mathbf{p}}_1(21)\cdot\Delta\mathbf{R}_1+\cdots, \tag{A27}$$

where

$$\overline{\mathbf{p}}_1(21)\equiv-\left(\frac{\partial S(\mathbf{r}_2,\overline{\mathbf{R}}_1;t_2)}{\partial\overline{\mathbf{R}}_1}\right)_{\mathbf{r}_2}, \tag{A28}$$

the initial momentum for a classical trajectory connecting $\overline{\mathbf{R}}_1$ and $\mathbf{r}_2$ in time t_2. At this stage

$$\overline{\mathbf{p}}_1(10)\neq\overline{\mathbf{p}}_1(21), \tag{A29}$$

so that the classical trajectory from $\overline{\mathbf{R}}_0$ to $\mathbf{r}_2$ via $\overline{\mathbf{R}}_1$ consists of two segments, with a momentum discontinuity at $\mathbf{r}=\overline{\mathbf{R}}_1$.

Applying the linearization approximation to Eq. (A22), we have

$$\begin{aligned}R^{(2)}(t_2,t_1)=&\left(\frac{i}{\hbar}\right)^2\frac{1}{(2\pi\hbar)^{2F}}\int d\mathbf{r}_2\int d\overline{\mathbf{R}}_1\int d\Delta\mathbf{R}_1\\&\times\int d\overline{\mathbf{R}}_0\int d\Delta\mathbf{R}_0\int d\mathbf{P}_0\rho_W(\overline{\mathbf{R}}_0,\mathbf{P}_0)\\&\times\left|\det\left[\frac{\partial\overline{\mathbf{p}}_1(21)}{\partial\mathbf{r}_2}\right]\right|\left|\det\left[\frac{\partial\overline{\mathbf{p}}_0}{\partial\overline{\mathbf{R}}_1}\right]\right|\\&\times e^{i(\overline{\mathbf{p}}_1(10)-\overline{\mathbf{p}}_1(21))\cdot\Delta\mathbf{R}_1/\hbar}e^{i(\mathbf{P}_0-\overline{\mathbf{p}}_0)\cdot\Delta\mathbf{R}_0/\hbar}\\&\times x_2\Delta X_1\Delta X_0.\end{aligned} \tag{A30}$$

Now noting

$$\begin{aligned}&\left(\frac{1}{i\hbar}\right)\frac{1}{(2\pi\hbar)^F}\int d\Delta\mathbf{R}_1\Delta X_1 e^{i(\overline{\mathbf{p}}_1(10)-\overline{\mathbf{p}}_1(21))\cdot\Delta\mathbf{R}_1/\hbar}\\&=\left[\frac{\partial\delta(\overline{p}_1(10)-\overline{p}_1(21))}{\partial\overline{p}_1(21)}\right]\prod_{\alpha=1}^{F-1}\delta(\overline{\mathbf{p}}_1(10)_\alpha-\overline{\mathbf{p}}_1(21)_\alpha)\end{aligned} \tag{A31}$$

and $x_2=x_2(\overline{\mathbf{R}}_1,\overline{\mathbf{p}}_1(21),t_2)$, and using Eq. (A13), we see that integration over $\Delta\mathbf{R}_1$ followed by integration over $\mathbf{r}_2$ imposes the condition,

$$\overline{\mathbf{p}}_1(10)=\overline{\mathbf{p}}_1(21)\equiv\overline{\mathbf{p}}_1. \tag{A32}$$

That is, the classical trajectory connecting $\overline{\mathbf{R}}_0$ to $\mathbf{r}_2$ via $\overline{\mathbf{R}}_1$ in time t_2+t_1 is now *continuous* in momentum at $\overline{\mathbf{R}}_1$. The expression for $R^{(2)}$ becomes

$$R^{(2)}(t_2,t_1)=-\left(\frac{1}{i\hbar}\right)\frac{1}{(2\pi\hbar)^F}\int d\overline{\mathbf{R}}_1\int d\overline{\mathbf{R}}_0\int d\Delta\mathbf{R}_0 \times\int d\mathbf{P}_0\rho_W(\overline{\mathbf{R}}_0,\mathbf{P}_0)\frac{\partial x_2(\overline{\mathbf{R}}_1,\overline{\mathbf{p}}_1;t_2)}{\partial\overline{p}_1} \times\left|\det\left[\frac{\partial\overline{\mathbf{p}}_0}{\partial\overline{\mathbf{R}}_1}\right]\right|e^{i(\mathbf{P}_0-\overline{\mathbf{p}}_0)\cdot\Delta\mathbf{R}_0/\hbar}\Delta X_0. \quad \text{(A33)}$$

The partial derivative

$$\frac{\partial x_2(\overline{\mathbf{R}}_1,\overline{\mathbf{p}}_1;t_2)}{\partial\overline{p}_1}=-\{x_2(\overline{\mathbf{R}}_1,\overline{\mathbf{p}}_1;t_2),\overline{X}_1(t_1)\} \quad \text{(A34)}$$

is the negative of the 2-time Poisson bracket of x_2 and $\overline{X}_1$.

Completing the integrations over $\Delta\mathbf{R}_0$ and $\overline{\mathbf{R}}_1$ as in the linear response case, we obtain the result,

$$R^{(2)}(t_2,t_1)=\int d\mathbf{R}_0\int d\mathbf{P}_0\frac{\partial}{\partial P_0}\left[\frac{\partial x_2(\overline{\mathbf{R}}_1,\overline{\mathbf{p}}_1;t_2)}{\partial\overline{p}_1}\right]\times\rho_W(\mathbf{R}_0,\mathbf{P}_0) \quad \text{(A35a)}$$

$$=\int d\mathbf{R}_0\int d\mathbf{P}_0\{\{x_2,\overline{X}_1\},X_0\}\rho_W(\mathbf{R}_0,\mathbf{P}_0). \quad \text{(A35b)}$$

Again, we have the multitime Poisson bracket weighted by the Wigner function ρ_W. Setting $\rho_W\simeq f_{\rm cl}$, we obtain the classical expression for the nonlinear response function as the equilibrium average of the multitime Poisson bracket $\{\{x_2,x_1\},x\}$.[11]

3. General case

The semiclassical approximation to the nth order response function $R^{(n)}(t_n,\ldots,t_1)$ is

$$R^{(n)}(t_n,\ldots,t_1)=\left(\frac{i}{\hbar}\right)^n\int d\mathbf{r}_n\int d\mathbf{r}'_{n-1}\int d\mathbf{r}''_{n-1}\cdots\int d\mathbf{r}'_1\int d\mathbf{r}''_1\int d\mathbf{R}_0\int d\mathbf{P}_0\int d\Delta\mathbf{R}_0K_{VV}(\mathbf{r}_n,\mathbf{r}'_{n-1};t_n)* \times K_{VV}(\mathbf{r}_n,\mathbf{r}''_{n-1};t_n)\cdots K_{VV}(\mathbf{r}'_1,\mathbf{r}'_0;t_1)*K_{VV}(\mathbf{r}''_1,\mathbf{r}''_0;t_1)x_n(x''_{n-1}-x'_{n-1})\cdots(x''_0-x'_0)\rho_W(\mathbf{R}_0,\mathbf{P}_0)e^{i\mathbf{P}_0\cdot\Delta\mathbf{R}_0/\hbar}. \quad \text{(A36)}$$

This expression involves determination of $n-1$ pairs of trajectories connecting $\mathbf{r}'_j\to\mathbf{r}'_{j+1}$ and $\mathbf{r}''_j\to\mathbf{r}''_{j+1}$ in time t_{j+1} and of a final pair of trajectories connecting $\mathbf{r}'_{n-1}\to\mathbf{r}_n$ and $\mathbf{r}''_{n-1}\to\mathbf{r}_n$ in time t_n Expansion of the product of n coordinate differences yields 2^n distinct terms.[10] The classical expression for the nonlinear response function $R^{(n)}$ is straightforwardly obtained from Eq. (A36) in the limit $\hbar\to0$ using the manipulations employed above.

Although both the HK (14) and Van Vleck (A36) expressions for the nth order response functions require the propagation of n trajectory pairs, the specification of the trajectories is different in each case. The HK expression integrates over the contributions from $2n$ trajectory segments, where each segment has independent initial conditions (coordinates and momenta). There is therefore a ''jump'' both in coordinate and momentum between trajectory segments. The $2n$ trajectories in the Van Vleck expression are specified by their initial and final coordinates, where the final coordinate of one trajectory is the intial coordinate of the next, so that only a momentum jump occurs between segments. This is true even when an IVR expression is used for the Van Vleck response function.

The integrations over intermediate coordinate pairs $\{\mathbf{r}''_j,\mathbf{r}'_j\}$ in Eq. (A36) can be performed by repeated use of the semiclassical concatenation formula,[18]

$$K_{VV}(\mathbf{r}_2,\mathbf{r}''_0;t_2+t_1)\overset{\rm SPA}{=}\int d\mathbf{r}''_1K_{VV}(\mathbf{r}_2,\mathbf{r}''_1;t_2)K_{VV}(\mathbf{r}''_1,\mathbf{r}''_0;t_1), \quad \text{(A37)}$$

where the integration over $\mathbf{r}''_1$ is performed by stationary phase, and the semiclassical propagator on the left-hand side of Eq. (A37) is evaluated for continuous (in momentum) trajectories connecting $\mathbf{r}''_0(t_0=0)$ to $\mathbf{r}_2(t_2+t_1)$. We thereby obtain

$$R^{(n)}(t_n,\ldots,t_1)=\left(\frac{i}{\hbar}\right)^n\int d\mathbf{r}_n\int d\mathbf{R}_0\int d\mathbf{P}_0\int d\Delta\mathbf{R}_0 \times\rho_W(\mathbf{R}_0,\mathbf{P}_0)e^{i\mathbf{P}_0\cdot\Delta\mathbf{R}_0/\hbar}K_{VV}(\mathbf{r}_n,\mathbf{r}'_0;T_n)* \times K_{VV}(\mathbf{r}_n,\mathbf{r}''_0;T_n)x_n(x''(T_{n-1}) -x'(T_{n-1}))\cdots(x''(T_1)-x'(T_1))(x''_0-x'_0), \quad \text{(A38)}$$

where $x''(T_k)$ is the value of the coordinate x at time $T_k\equiv t_1+t_2+\cdots+t_k$ along the *continuous* (in momentum) classical trajectory connecting x''_0 at $t_0=0$ with x_n at $t=T_n$, and similarly for $x'_1(T_k)$. Expression (A38) is an approximate version of Eq. (A36); the momentum matching conditions at times T_k constrain the trajectories from $\mathbf{r}''_0$ and $\mathbf{r}'_0$ to $\mathbf{r}_n$ to be continuous in phase space, so that numerical evaluation of Eq. (A38) for the nonlinear response function of any order is comparable in difficulty to calculation of the linear response function from Eq. (A7).

APPENDIX B: CONSEQUENCES OF EQ. (34)

We explore here several consequences of the exact relation involving coherent states overlaps in Eq. (34), one of which is the result in Eq. (26), which was employed to show that the semiclassical expression for the linear response func-

tion in Eq. (15) is exactly correct for a harmonic system. The result in Eq. (34) may be written as an operator identity,

$$\int \frac{d\overline{\mathbf{z}}_{ij}}{(2\pi\hbar)^F} \frac{|\mathbf{z}_j\rangle\langle\mathbf{z}_i|}{\langle\mathbf{z}_i|\mathbf{z}_j\rangle} = \hat{\mathbf{I}}, \tag{B1}$$

with $\hat{\mathbf{I}}$ The identity operator. The relation in Eq. (26) follows, according to

$$\begin{aligned}\int \frac{d\overline{\mathbf{z}}_{ij}}{(2\pi\hbar)^F} \frac{\langle\mathbf{z}_i|\hat{\rho}|\mathbf{z}_j\rangle}{\langle\mathbf{z}_i|\mathbf{z}_j\rangle} &= \int \frac{d\overline{\mathbf{z}}_{ij}}{(2\pi\hbar)^F} \mathrm{Tr}\left[\frac{|\mathbf{z}_j\rangle\langle\mathbf{z}_i|}{\langle\mathbf{z}_i|\mathbf{z}_j\rangle}\hat{\rho}\right] \\ &= \mathrm{Tr}\left[\int \frac{d\overline{\mathbf{z}}_{ij}}{(2\pi\hbar)^F} \frac{|\mathbf{z}_i\rangle\langle\mathbf{z}_j|}{\langle\mathbf{z}_i|\mathbf{z}_j\rangle}\hat{\rho}\right] \\ &= \mathrm{Tr}\,\hat{\rho}. \end{aligned} \tag{B2}$$

The identity in Eq. (B1) may be written more compactly, and so, therefore, may the semiclassical nonlinear response function in Eq. (10), by introducing coherent states associated with complex-valued coordinates and momenta. We define $|\tilde{\mathbf{z}}_{ij}\rangle$, a coherent state associated with a complex-valued phase point connected with the phase points $\mathbf{z}_i$ and $\mathbf{z}_j$ according to

$$\begin{aligned} |\tilde{\mathbf{z}}_{ij}\rangle &\equiv \left|\frac{\langle\mathbf{z}_i|\hat{\mathbf{q}}|\mathbf{z}_j\rangle}{\langle\mathbf{z}_i|\mathbf{z}_j\rangle}, \frac{\langle\mathbf{z}_i|\hat{\mathbf{p}}|\mathbf{z}_j\rangle}{\langle\mathbf{z}_i|\mathbf{z}_j\rangle}\right\rangle. \\ \langle\tilde{\mathbf{z}}^*_{ij}| &\equiv \left\langle\left(\frac{\langle\mathbf{z}_i|\hat{\mathbf{q}}|\mathbf{z}_j\rangle}{\langle\mathbf{z}_i|\mathbf{z}_j\rangle}\right)^*, \left(\frac{\langle\mathbf{z}_i|\hat{\mathbf{p}}|\mathbf{z}_j\rangle}{\langle\mathbf{z}_i|\mathbf{z}_j\rangle}\right)^*\right|, \end{aligned} \tag{B3}$$

$$\begin{aligned} \frac{\langle\mathbf{z}_i|\hat{\mathbf{q}}|\mathbf{z}_j\rangle}{\langle\mathbf{z}_i|\mathbf{z}_j\rangle} &= \overline{\mathbf{q}}_{ij} - \frac{i}{2\hbar\gamma}\Delta\mathbf{p}_{ij}, \\ \frac{\langle\mathbf{z}_i|\hat{\mathbf{p}}|\mathbf{z}_j\rangle}{\langle\mathbf{z}_i|\mathbf{z}_j\rangle} &= \overline{\mathbf{p}}_{ij} + \frac{i\hbar\gamma}{2}\Delta\mathbf{q}_{ij}. \end{aligned} \tag{B4}$$

The coherent state coordinate and momentum are analytically continued to the complex-valued quantities in Eq. (B4). The motivation for these definitions arises from the following relations, which may, for example, be verified by taking inner products with coordinate states,

$$\begin{aligned} |\tilde{\mathbf{z}}_{ij}\rangle &= \frac{|\mathbf{z}_j\rangle}{\sqrt{\langle\mathbf{z}_i|\mathbf{z}_j\rangle}} \exp\left[-\frac{1}{\hbar^2\gamma}\overline{\mathbf{p}}_{ij}\cdot\Delta\mathbf{p}_{ij}\right], \\ \langle\tilde{\mathbf{z}}^*_{ij}| &= \frac{\langle\mathbf{z}_i|}{\sqrt{\langle\mathbf{z}_i|\mathbf{z}_j\rangle}} \exp\left[\frac{1}{\hbar^2\gamma}\overline{\mathbf{p}}_{ij}\cdot\Delta\mathbf{p}_{ij}\right]. \end{aligned} \tag{B5}$$

Assembling the ket and bra from Eqs. (B5) produces

$$|\tilde{\mathbf{z}}_{ij}\rangle\langle\tilde{\mathbf{z}}^*_{ij}| = \frac{|\mathbf{z}_j\rangle\langle\mathbf{z}_i|}{\langle\mathbf{z}_i|\mathbf{z}_j\rangle}. \tag{B6}$$

This identity provides a convenient formulation for the off-diagonal matrix element between coherent states of any operator $\hat{A}$,

$$\langle\mathbf{z}_i|\hat{A}|\mathbf{z}_j\rangle = \langle\mathbf{z}_i|\mathbf{z}_j\rangle\langle\tilde{\mathbf{z}}^*_{ij}|\hat{A}|\tilde{\mathbf{z}}_{ij}\rangle. \tag{B7}$$

Our formulation of the semiclassical response function is based on the relation in Eq. (8) for the coherent states matrix element of a commutator with the coordinate operator. This result may be written in terms of coherent states for complex phase points as

$$\langle\mathbf{z}_i|[\hat{x},\hat{A}]|\mathbf{z}_j\rangle = i\hbar\langle\mathbf{z}_i|\mathbf{z}_j\rangle\frac{\partial}{\partial\overline{p}_{ij}}(\langle\tilde{\mathbf{z}}^*_{ij}|\hat{A}|\tilde{\mathbf{z}}_{ij}\rangle), \tag{B8}$$

which leads to a more compact formulation of the response function in Eq. (10),

$$\begin{aligned} R^{(n)}(t_n,\ldots,t_1) = (-1)^n \int \frac{d\mathbf{z}_1}{(2\pi\hbar)^F} \int \frac{d\mathbf{z}_2}{(2\pi\hbar)^F} \cdots \int \frac{d\mathbf{z}_{2n}}{(2\pi\hbar)^F} G(\mathbf{z}_1,t_1)G^*(\mathbf{z}_2,t_1)\cdots G(\mathbf{z}_{2n-1},t_n) \\ \times G^*(\mathbf{z}_{2n},t_n)\left\{\langle\mathbf{z}_{2n}(t_n)|\mathbf{z}_{2n-1}(t_n)\rangle\left[\overline{q}_{2n-1,2n}(t_n) + \frac{i}{2\hbar\gamma}\Delta p_{2n-1,2n}(t_n)\right]\right\} \\ \times\left\{\langle\mathbf{z}_{2n-1}|\mathbf{z}_{2n}\rangle\left[\frac{\partial}{\partial\overline{p}_{2n-1,2n}}(\langle\mathbf{z}_{2n-2}(t_{n-1})|\tilde{\mathbf{z}}_{2n-1,2n}\rangle\langle\tilde{\mathbf{z}}^*_{2n-1,2n}|\mathbf{z}_{2n-3}(t_{n-1})\rangle)\right]\right\} \\ \times\left\{\langle\mathbf{z}_{2n-3}|\mathbf{z}_{2n-2}\rangle\left[\frac{\partial}{\partial\overline{p}_{2n-3,2n-2}}(\langle\mathbf{z}_{2n-4}(t_{n-2})|\tilde{\mathbf{z}}_{2n-3,2n-2}\rangle\langle\tilde{\mathbf{z}}^*_{2n-3,2n-2}|\mathbf{z}_{2n-5}(t_{n-2})\rangle)\right]\right\}\cdots \\ \times\left\{\langle\mathbf{z}_3|\mathbf{z}_4\rangle\left[\frac{\partial}{\partial\overline{p}_{34}}(\langle\mathbf{z}_2(t_1)|\tilde{\mathbf{z}}_{34}\rangle\langle\tilde{\mathbf{z}}^*_{34}|\mathbf{z}_1(t_1)\rangle)\right]\right\}\langle\mathbf{z}_1|\mathbf{z}_2\rangle\frac{\partial}{\partial\overline{p}_{12}}(\langle\tilde{\mathbf{z}}^*_{12}|\hat{\rho}|\tilde{\mathbf{z}}_{12}\rangle). \end{aligned} \tag{B9}$$

The overlaps between conventional and complexified coherent states may be evaluated using straightforward analytical continuation of the appropriate coordinates and momenta, and the momentum derivatives may be evaluated explicitly to produce a relation analogous to Eq. (14). The identity in Eq. (B1) may be reformulated as a completeness relation for complexified coherent states,

$$\int \frac{d\overline{\mathbf{z}}_{ij}}{(2\pi\hbar)^F} |\tilde{\mathbf{z}}_{ij}\rangle\langle\tilde{\mathbf{z}}^*_{ij}| = \hat{\mathbf{I}}, \tag{B10}$$

which is useful in manipulations with $R^{(n)}$ as expressed in Eq. (B9).

APPENDIX C: VERIFICATION OF EQ. (27)

The extraction of the correct classical mechanical limit from the semiclassical nonlinear response function in Eq. (10) relies on the identity in Eq. (27), which we verify here. This identity has previously been proven by Herman and Coker,[47] and stated by Wang, Manolopoulos, and Miller[56] [see Eqs. (A9) and (A11) of Ref. 56].

Substitution of the relation in Eq. (20) into Eq. (27) permits the latter identity to be rewritten as

$$|C(\overline{\mathbf{z}}_{12},t)|^2 \int \frac{d\Delta\mathbf{Z}_{12}}{(2\pi)^F} \exp\left[-\frac{1}{4}\Delta\mathbf{Z}_{12}^T\cdot\mathbf{W}\cdot\Delta\mathbf{Z}_{12}\right]=1, \tag{C1}$$

$$\mathbf{W}=\mathbf{I}_{2F}+\overline{\mathbf{M}}^T\cdot\overline{\mathbf{M}}. \tag{C2}$$

The $2F$-dimensional matrix $\overline{\mathbf{M}}$ is the dimensionless monodromy matrix defined in Eq. (21). Evaluation of this Gaussian integral gives

$$\frac{2^F|C(\overline{\mathbf{z}}_{12},t)|^2}{\sqrt{\det\mathbf{W}}}=1. \tag{C3}$$

We express the HK prefactor $C(\mathbf{z},t)$ in Eq. (5) as

$$C(\mathbf{z},t)\equiv\sqrt{\det\mathbf{\Lambda}}. \tag{C4}$$

The identity to be verified in Eq. (27) then takes the form,

$$\det\mathbf{W}=2^{2F}\det(\mathbf{\Lambda}^\dagger\mathbf{\Lambda}). \tag{C5}$$

To verify the equality in Eq. (C5), we write $\mathbf{W}$ as a product of $2F$-dimensional matrices $\mathbf{U}$ and $\mathbf{V}$,

$$\mathbf{W}=\mathbf{U}\cdot\mathbf{V}, \tag{C6}$$

$$\mathbf{U}=\begin{bmatrix}\mathbf{\Lambda}^T & \mathbf{\Lambda}^\dagger\\ i\mathbf{\Lambda}^T & -i\mathbf{\Lambda}^\dagger\end{bmatrix}, \tag{C7}$$

$$\mathbf{V}=\begin{bmatrix}\mathbf{M}_{qq}(\overline{\mathbf{z}},t)-i(\hbar\gamma)^{-1}\mathbf{M}_{pq}(\overline{\mathbf{z}},t) & \hbar\gamma\mathbf{M}_{qp}(\overline{\mathbf{z}},t)-i\mathbf{M}_{pp}(\overline{\mathbf{z}},t)\\ \mathbf{M}_{qq}(\overline{\mathbf{z}},t)+i(\hbar\gamma)^{-1}\mathbf{M}_{pq}(\overline{\mathbf{z}},t) & \hbar\gamma\mathbf{M}_{qp}(\overline{\mathbf{z}},t)+i\mathbf{M}_{pp}(\overline{\mathbf{z}},t)\end{bmatrix}. \tag{C8}$$

The demonstration that $\mathbf{W}=\mathbf{U}\cdot\mathbf{V}$, not shown here, requires invoking the symplectic property of the monodromy matrix,

$$\overline{\mathbf{M}}\cdot\mathbf{J}\cdot\overline{\mathbf{M}}^T=\mathbf{J}, \tag{C9}$$

$$\mathbf{J}=\begin{bmatrix}\mathbf{0}_F & \mathbf{I}_F\\ -\mathbf{I}_F & \mathbf{0}_F\end{bmatrix}, \tag{C10}$$

with $\mathbf{0}_F$ the F-dimensional matrix with all elements zero.

By two successive manipulations of adding a multiple of one row of the matrix to another, the determinant of $\mathbf{U}$ can be written as

$$\det\mathbf{U}=(-2i)^F\det\begin{bmatrix}\mathbf{\Lambda}^T & \mathbf{0}_F\\ \mathbf{0}_F & \mathbf{\Lambda}^\dagger\end{bmatrix}$$
$$=(-2i)^F\det\mathbf{\Lambda}^T\det\mathbf{\Lambda}^\dagger=(-2i)^F\det(\mathbf{\Lambda}^\dagger\mathbf{\Lambda}). \tag{C11}$$

Similarly, by twice adding a multiple of one row to another in $\mathbf{V}$, its determinant can be put in the form,

$$\det\mathbf{V}=(2i)^F\det\overline{\mathbf{M}}=(2i)^F, \tag{C12}$$

where the unit determinant of the monodromy matrix has been invoked. Multiplying the determinants of $\mathbf{U}$ and $\mathbf{V}$ in Eqs. (C11) and (C12) produces the desired result in Eq. (C5).

[1] S. Mukamel, A. Piryatinski, and V. Chernyak, Acc. Chem. Res. **32**, 145 (1999).
[2] M. D. Fayer, Annu. Rev. Phys. Chem. **52**, 315 (2001).
[3] K. A. Merchant, D. E. Thompson, Q.-H. Xu, R. B. Williams, R. F. Loring, and M. D. Fayer, Biophys. J. **82**, 3277 (2002).
[4] K. A. Merchant, W. G. Noid, D. E. Thompson, R. Akiyama, R. F. Loring, and M. D. Fayer, J. Phys. Chem. B **107**, 4 (2003).
[5] P. Hamm, M. Lim, and R. M. Hochstrasser, Phys. Rev. Lett. **81**, 5326 (1998).
[6] M. T. Zanni and R. M. Hochstrasser, Curr. Opin. Struct. Biol. **11**, 516 (2001).
[7] J. C. Wright, Int. Rev. Phys. Chem. **21**, 185 (2002).
[8] O. Golonzka, M. Khalil, N. Demirdoven, and A. Tokmakoff, J. Chem. Phys. **115**, 10814 (2001).
[9] J. Stenger, D. Madsen, P. Hamm, E. T. J. Nibbering, and T. Elsaesser, J. Phys. Chem. A **106**, 2341 (2002).
[10] S. Mukamel, *Principles of Nonlinear Optical Spectroscopy* (Oxford University Press, New York, 1995).
[11] S. Mukamel, V. Khidekel, and V. Chernyak, Phys. Rev. E **53**, R1 (1996).
[12] R. B. Williams and R. F. Loring, J. Chem. Phys. **113**, 1932 (2000).
[13] R. B. Williams and R. F. Loring, J. Chem. Phys. **113**, 10651 (2000).
[14] R. B. Williams and R. F. Loring, Chem. Phys. **266**, 167 (2001).
[15] R. Akiyama and R. F. Loring, J. Chem. Phys. **116**, 4655 (2002).
[16] R. Akiyama and R. F. Loring, J. Phys. Chem. A (to be published).
[17] J. H. Van Vleck, Proc. Natl. Acad. Sci. U.S.A. **14**, 178 (1928).
[18] M. V. Berry and K. E. Mount, Rep. Prog. Phys. **35**, 315 (1972).
[19] W. H. Miller, Adv. Chem. Phys. **XXV**, 69 (1974).
[20] W. H. Miller, Adv. Chem. Phys. **XXX**, 77 (1975).
[21] M. F. Herman and E. Kluk, Chem. Phys. **91**, 27 (1984).
[22] M. F. Herman, Annu. Rev. Phys. Chem. **45**, 83 (1994).
[23] M. C. Gutzwiller, *Chaos in Classical and Quantum Mechanics* (Springer-Verlag, New York, 1990).
[24] M. S. Child, *Semiclassical Mechanics with Molecular Applications* (Oxford University Press, New York, 1991).
[25] E. J. Heller, J. Chem. Phys. **94**, 2723 (1991).
[26] E. J. Heller, in *Chaos and Quantum Physics*, edited by M.-J. Giannoni, A. Voros, and J. Zinn-Justin (Elsevier, New York, 1991), pp. 549–663.
[27] M. A. Sepulveda and F. Grossmann, Adv. Chem. Phys. **XCVI**, 191 (1996).
[28] D. J. Tannor and S. Garashchuk, Annu. Rev. Phys. Chem. **51**, 553 (2000).
[29] W. H. Miller, J. Phys. Chem. A **105**, 2942 (2001).
[30] M. Baranger, M. A. M. de Aguiar, F. Keck, H. J. Korsch, and B. Schellhaass, J. Phys. A **34**, 7227 (2001).
[31] A. J. Lichtenberg and M. A. Lieberman, *Regular and Chaotic Dynamics* 2nd ed. (Springer Verlag, New York, 1992).
[32] L. S. Schulman, *Techniques and Applications of Path Integration* (Wiley, New York, 1981).
[33] R. E. Gillilan and K. R. Wilson, J. Chem. Phys. **97**, 1757 (1992).
[34] D. Passerone and M. Parrinello, Phys. Rev. Lett. **87**, 108302 (2001).
[35] W. H. Miller, J. Chem. Phys. **53**, 3578 (1970).
[36] R. A. Marcus, J. Chem. Phys. **56**, 3548 (1972).

[37] W. H. Miller, J. Chem. Phys. **95**, 9428 (1991).
[38] K. G. Kay, J. Chem. Phys. **100**, 4377 (1994).
[39] K. G. Kay, J. Chem. Phys. **100**, 4432 (1994).
[40] K. G. Kay, J. Chem. Phys. **101**, 2250 (1994).
[41] E. J. Heller, J. Chem. Phys. **75**, 2923 (1981).
[42] J. R. Klauder and B. Skagerstam, *Coherent States: Applications in Physics and Mathematical Physics* (World Scientific, Singapore, 1985).
[43] R. G. Littlejohn, Phys. Rep. **138**, 193 (1986).
[44] F. Grossmann and A. L. Xavier, Phys. Lett. A **243**, 243 (1998).
[45] W. H. Miller, Mol. Phys. **100**, 397 (2002).
[46] W. H. Miller, J. Phys. Chem. B **106**, 8132 (2002).
[47] M. F. Herman and D. F. Coker, J. Chem. Phys. **111**, 1801 (1999).
[48] J. Cao and G. A. Voth, J. Chem. Phys. **104**, 273 (1996).
[49] R. Hernandez and G. A. Voth, Chem. Phys. **233**, 243 (1998).
[50] X. Sun and W. H. Miller, J. Chem. Phys. **110**, 6635 (1999).
[51] K. Thompson and N. Makri, Phys. Rev. E **59**, 4729 (1999).
[52] J. Shao and N. Makri, J. Phys. Chem. A **103**, 7753 (1999).
[53] Y. Zhao and N. Makri, Chem. Phys. **280**, 135 (2002).
[54] J. L. McWhirter, J. Chem. Phys. **112**, 7891 (2000).
[55] J. Wu and J. Cao, J. Chem. Phys. **115**, 5381 (2001).
[56] H. Wang, D. E. Manolopoulos, and W. H. Miller, J. Chem. Phys. **115**, 6317 (2001).
[57] C. Jaffe and P. Brumer, J. Chem. Phys. **73**, 5646 (1980).
[58] R. B. Shirts, J. Phys. Chem. **91**, 2258 (1987).
[59] N. Makri and W. H. Miller, J. Chem. Phys. **116**, 9207 (2002).
[60] S. X. Sun and W. H. Miller, J. Chem. Phys. **117**, 5522 (2002).
[61] M. Allen and D. Tildesley, *Computer Simulation of Liquids* (Oxford University Press, New York, 1996).
[62] M. F. Herman, J. Chem. Phys. **85**, 2069 (1986).
[63] J. A. Leegwater and S. Mukamel, J. Chem. Phys. **102**, 2365 (1995).
[64] H. B. Wang, X. Sun, and W. H. Miller, J. Chem. Phys. **108**, 9726 (1998).
[65] M. A. Sepulveda and S. Mukamel, J. Chem. Phys. **102**, 9327 (1995).
[66] V. Khidekel, V. Chernyak, and S. Mukamel, in *Femtochemistry: Ultrafast Chemical and Physical Processes in Molecular Systems*, edited by M. Chergui (World Scientific, Singapore, 1996), pp. 507–514.
[67] S. Mukamel, Phys. Rev. A **61**, 021804 (2000).
[68] M. Hillery, R. F. O'Connell, M. O. Scully, and E. P. Wigner, Phys. Rep. **106**, 121 (1984).